Geological Quarterly, 2022, 66: 21
DOI: http://dx.doi.org/10.7306/gq.1653

Detrital zircon analysis of metasedimentary rocks of the Staré Město Belt, Sudetes: implications for the provenance and evolution of the eastern margin of the Saxothuringian terrane, NE Bohemian Massif

Marek ŚLIWIŃSKI[1, *], Mirosław JASTRZĘBSKI[1] and Jiří SLÁMA[2]

[1] Polish Academy of Sciences, Institute of Geological Sciences, Research Centre in Wrocław, Podwale 75, 50-449 Wrocław, Poland

[2] Czech Academy of Sciences, Institute of Geology, Rozvojová 269, 165 00, Praha 6 – Lysolaje, Czech Republic

Śliwiński, M., Jastrzębski, M., Sláma, J., 2022. Detrital zircon analysis of metasedimentary rocks of the Staré Město Belt, Sudetes: implications for the provenance and evolution of the eastern margin of the Saxothuringian terrane, NE Bohemian Massif. Geological Quarterly, 66: 21, doi: 10.7306/gq.1653

Associate Editor: Leszek Krzemiński

The Staré Město Belt (SMB) in the Central Sudetes forms a Variscan tectonic boundary zone that is located between the Saxothuringian and Brunovistulian terranes of the Bohemian Massif. The three thrust-bounded upper, middle and lower lithotectonic units of the SMB are composed of metasedimentary and Late Cambrian metavolcanic rocks. A new LA-ICP-MS zircon geochronology supported by zircon typology studies of the mica schists of the upper unit and the migmatitic paragneisses of the middle unit provides new insights into the provenance and evolution of the SMB. Our new data were obtained from metasedimentary rocks and compared to the previously published zircon ages of the SMB metavolcanic rocks. The results indicate that the metasedimentary and bimodal metavolcanic rocks in the separate lithotectonic units of the SMB originally formed Late Cambrian volcano-sedimentary successions. The source areas of the sedimentary basins studied were dominated by Neoproterozoic and Paleoproterozoic crystalline rocks that were presumably located near the West African Craton of Gondwana. A comparison of the detrital age spectra obtained with those previously published from the region indicates a strong association of the entire SMB with the Saxothuringian terrane of the Bohemian Massif. During partial melting of the metasedimentary rocks of the middle unit of the SMB, Cambrian and older zircon grains were affected by solid-state transformations that caused partial resetting of the U-Pb dates, changes in internal zircon textures and reductions in Th/U ratios.

Key words: detrital zircon age spectra, provenance, Variscan terranes, Staré Město Belt, Bohemian Massif.

INTRODUCTION

The Sudetes, NW Bohemian Massif is a collage geological structure that consists of separate tectonostratigraphic units correlated with the major tectonic zones (microplates) of the Bohemian Massif that were juxtaposed during Variscan times (Cymerman et al., 1997; Franke and Żelaźniewicz 2000; Aleksandrowski and Mazur, 2002; Mazur et al., 2006; Fig. 1A). An important component of these units comprises the metavolcanic-sedimentary rocks that are remnants of pre-Variscan volcano-sedimentary successions. Such a rock association also occurs in the Staré Město Belt (SMB) in the Central Sudetes (Fig. 1B), which forms a tectonic boundary zone between the Saxothuringian and Brunovistulian terranes. The SMB is characterized by a predominance of metavolcanic rocks (e.g., Skácel, 1977; Štípská et al., 2001; Don et al., 2003) that represent a metamorphosed ophiolite sequence (e.g., Poubová and Sokol, 1992). The SMB metabasites originated in an ensialic rift setting (Floyd et al., 1996, 2000) that developed in the Cambro-Ordovician (Kröner et al., 2000; Fig. 1B).

Zircon geochronology studies suggest some differences in the provenance of the units that are present on both sides of the SMB. The source areas for the detrital materials for the metavolcanic-sedimentary successions are thought to lie within the Saxothuringian terrane, including those of the Orlica-Śnieżnik Dome, and are generally linked to the West African Craton of northern Gondwana (e.g., Linneman et al., 2004; Jastrzębski et al., 2010; Mazur et al., 2012; Oberc-Dziedzic et al., 2018; Szczepański et al., 2020). The Velké Vrbno Dome of the Brunovistulian terrane has been recently postulated to represent the Amazonian margin of Gondwana (Jastrzębski et al., 2021), but besides Gondwanan origin, a Baltican derivation is also suggested (Collett et al., 2021). The detrital zircon age spectra of the SMB are limited to those obtained from Brusek quartzites from the eastern part of the belt, which suggests the

* Corresponding author, e-mail: marek.sliwinski@twarda.pan.pl

Received: February 16, 2022; accepted: June 30, 2022; first published online: July 22, 2022

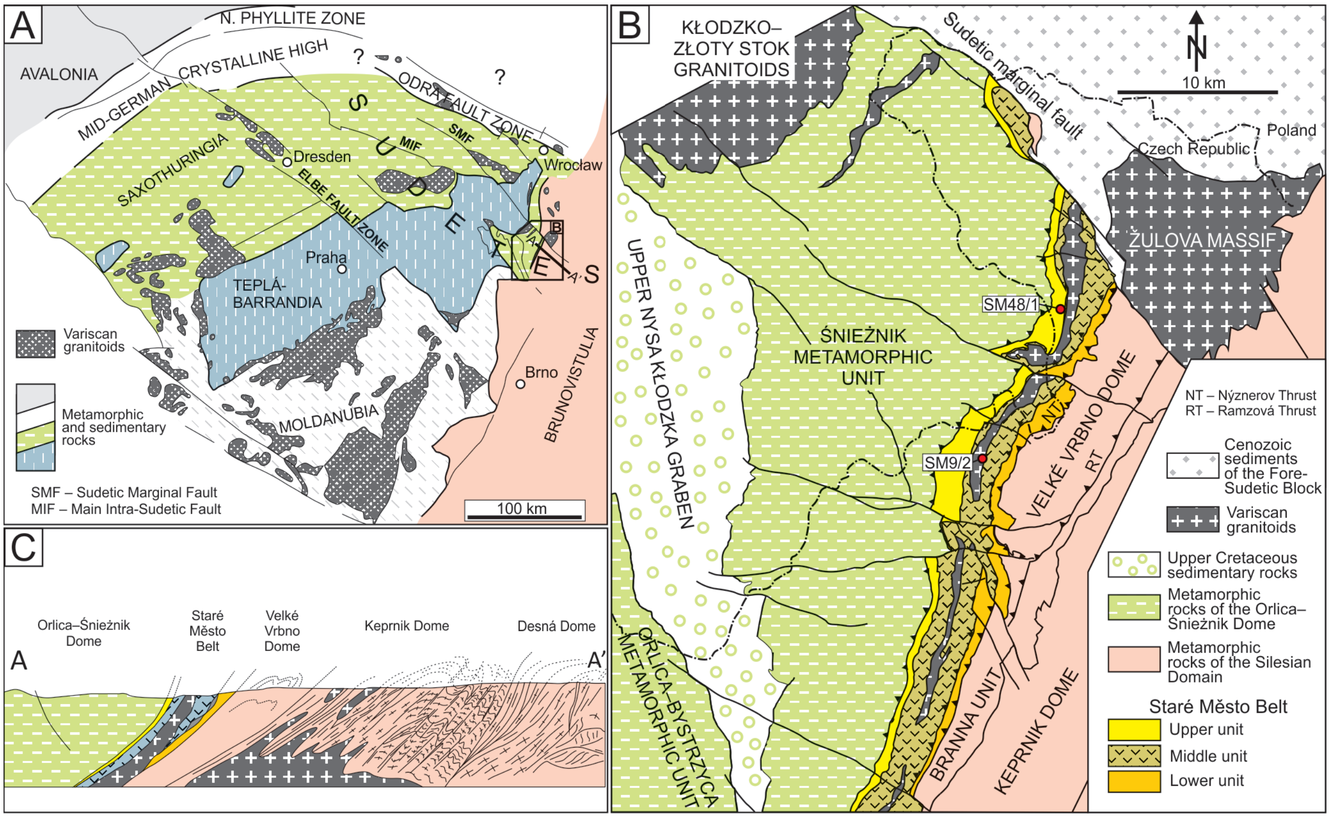

Fig. 1A – tectonic map of the Bohemian Massif (modified from Oberc-Dziedzic et al., 2015); B – position of the Staré Město Belt and the location of the samples studied on a geological sketch of the Central Sudetes (modified after Don et al., 2003); C – schematic cross-section through the Central Sudetes (modified from Schulmann and Gayer, 2000)

Saxothuringian affinity of these rocks (Jastrzębski et al., 2015). The SMB is, however, an internally complex fold-and-thrust belt, in which separate lithotectonic sheets contain large-scale tectonic boundaries (Don et al., 2003; Opletal and Pecina, 2004; Fig. 1B, C) which are suggestive of significant-scale juxtaposition within the SMB. Thus, the issue of whether the whole SMB, and its central, mainly metavolcanic part representing the presumed rift, in particular, was connected closer to the Saxothuringian or Brunovistulian terrane at the time of formation of the protoliths of the SMB metamorphic rocks requires more provenance data.

In this study, we provide new detrital zircon U-Pb data supported by zircon morphological analysis of metasedimentary rocks that represent two different lithotectonic portions of the SMB. The detrital zircon age spectra of these rocks have not previously been studied. The zircon data obtained from mica schist samples of the SMB upper unit and migmatitic paragneisses of the SMB middle unit have been compared with those obtained earlier in neighboring domains of the Saxothuringian and Brunovistulian terranes. The results provide necessary evidence for the provenance and significance of the Staré Město Belt within the Variscan structure of the Sudetes.

GEOLOGICAL BACKGROUND AND PREVIOUS ZIRCON GEOCHRONOLOGY

The Staré Město Belt is a 50 km-long and 2.5 to 4.5 km-wide, narrow tectonic zone with an SSW–NNE alignment and mainly has a moderate-angle westerly dip (Fig. 1). The SMB separates the Orlica–Śnieżnik Dome in the west from the Velké Vrbno Dome and Branná Belt in the east (Don et al., 2003). In this area, a major geological boundary dividing two domains with distinct geological characteristics was postulated nearly 100 years ago (e.g., Cloos, 1922; Bederke, 1929), and its exact position and significance have been discussed extensively since that time (e.g., Oberc, 1968; Cymerman, 1993; Schulmann and Gayer, 2000; Opletal and Pecina, 2004; Jastrzębski et al., 2015). In the modern tectonic subdivision of the Bohemian Massif, the Orlica–Śnieżnik Dome is usually considered to be part of the Saxothuringian terrane (e.g., Franke and Żelaźniewicz, 2000; Chopin et al., 2012; Aguilar et al., 2020), although it is sometimes considered to be part of the Moldanubian terrane (Matte et al., 1990; Cymerman et al., 1997). The Velké Vrbno Dome and Branná Belt belong to the Silesian domain, which is the northwestern part of the Brunovistulian (Brunia) microplate (e.g., Schulmann and Gayer, 2000; Štípská et al., 2006; Jastrzębski et al., 2015; Oberc-Dziedzic et al., 2021; Collett et al., 2021; Fig. 1A).

Geological mapping studies (e.g., Skácel, 1977; Gawlikowska and Opletal, 1997; Don et al., 2003) indicate that the upper and lower parts of the SMB are dominated by metasedimentary rocks, while the middle part is mainly composed of metavolcanic rocks (Fig. 1C). These narrow lithotectonic units are separated by west-dipping thrusts (e.g., Poubová and Sokol, 1992; Gawlikowska and Opletal, 1997; Don et al., 2003; Opletal and Pecina, 2004) and are defined as the upper, middle and lower units of the SMB, respectively (Jastrzębski, 2012).

The upper 1–3 km wide lithotectonic unit, which is equivalent to the "Hranična series" (Skácel, 1977, 1989), contains mostly metasedimentary rocks, such as mica schists interlayered with felsic and mafic metavolcanic rocks, graphite schists, marbles and quartzites (e.g., Skácel, 1977; Don et al., 2003; Fig. 1). The protolith ages of the felsic metavolcanic rocks from the upper unit have yielded a Pb-Pb zircon evaporation age of ~522 Ma (Kröner et al., 2000) and SHRIMP concordia age of ~493 Ma (Jastrzębski et al., 2015).

The metavolcanic rocks of the SMB are concentrated in up to 4 km-thick sections of the middle part of the belt. In this part of the SMB, the dominant rocks are amphibolites and quartzo-feldspathic rocks (Don et al. 2003). Paragneisses, metagabbros and boudins derived from serpentinized spinel peridotite are less common (Poubová and Sokol, 1992; Štípská et al., 2001). In most cases, the mafic and felsic metavolcanic rocks form sequences called bimodal associations. The geochemistry of the metabasites derived from those leptyno-amphibolite sequences indicates their MORB-like (Floyd et al., 1996, 2000) or island arc affinity (Poubová and Sokol, 1992). Floyd et al. (1996, 2000) considered that all chemical variations suggesting a subduction-related origin of these rocks are the result of crustal contamination of more primitive magmas that developed in an ensialic rift setting. The dating results for zircons from the metatonalites, metagabbros and metavolcanic rocks of the leptyno-amphibolite complex yield identical vapor digestion upper intercept ages, Pb-Pb evaporation mean ages and SHRIMP mean ages that range between ~505 and 503 Ma (Kröner et al., 2000). In this part of the SMB, which is defined as the SMB middle unit (Jastrzębski, 2012), smaller elongated bodies of migmatitic paragneiss also occur (Don et al., 2003). Dating of two detrital zircons from the granulite-facies paragneisses from the middle unit yielded SHRIMP ages of ~551 and ~609 Ma (Kröner et al., 2000). The examination of two other zircons from this rock provided Pb-Pb evaporation ages of ~664 and ~682 Ma (Kröner et al., 2000). Multifaceted zircon grains from the same sample yielded 504–509 Ma ages (U-Pb SHRIMP mean age and upper intercept age were derived by vapor digestion), which were interpreted as reflecting the timing of high-grade metamorphic conditions in this part of the SMB (Kröner et al., 2000).

The SMB lower unit, which has a thickness of ~800 m, is lithologically more similar to the upper unit because of the predominance of metasedimentary rocks over metavolcanic rocks. This unit is mainly composed of mica schists termed the Skorošice mica schist by Don et al. (2003) and also contains cataclased gneisses, amphibolites, marbles, quartzites, and graphite schists (Don et al., 2003). A felsic metavolcanic rock in the lower unit yielded a protolith age of ~498 Ma (U–Pb SHRIMP zircon dating, Jastrzębski et al., 2015). A SHRIMP detrital zircon study on the Brusek quartzites at the bottom of the SMB lower unit indicates the presence of two Neoproterozoic–Early Cambrian (672 to 531 Ma) and Paleoproterozoic (2.19–1.96 Ga and 2.47 Ga) age clusters that are suggestive of a Saxothuringian provenance (Jastrzębski et al., 2015).

The Lower Paleozoic rocks of the SMB were metamorphosed under amphibolite- to granulite-facies conditions (e.g., Parry et al., 1997; Štípská et al., 2001; Bartz, 2004; Lexa et al., 2005), either during the Cambro-Ordovician and/or Devono-Carboniferous (see Lexa et al., 2005; Jastrzębski et al., 2013). The main structural architecture of the SMB was established during Visean time (340–344 Ma), when the metamorphic rocks were intruded by syntectonic tonalite-granodiorite sheet intrusions (e.g., Wierzchołowski, 1966; Parry et al., 1997; Štípská et al., 2004; Jastrzębski et al., 2018).

METHODS

The zircons from the SM48/1 mica schist and SM9/2 paragneiss were separated using standard techniques, including crushing, magnetic separation and handpicking under a binocular microscope. Despite the metasedimentary origin of the rocks studied, the typological classification of Pupin (1980) was applied to the zircon grains from both samples studied. Secondary electron images (SEM) of representative morphological subtypes of zircon grains were obtained using a *Jeol JSM-IT500LA* scanning electron microscope at the Electron Microscopy Laboratory of the Institute of Geological Sciences, University of Wrocław, Poland.

The zircon grains were mounted in epoxy resin, polished and imaged with cathodoluminescence (CL) before the isotopic analysis. A Thermo Scientific Element 2 sector field ICP–MS coupled to a 193 nm ArF excimer laser (*Teledyne Cetac Analyte Excite* laser) at the Institute of Geology of the Czech Academy of Sciences, Prague, Czech Republic, was used to determine the zircon Pb/U and Pb isotope ratios. Details of the analytical techniques are provided in Appendix (Table S1). In the results presented below, zircon ages younger than 1 Ga are $^{206}Pb/^{238}U$ ages and U-Pb ages older than 1 Ga are $^{207}Pb/^{206}Pb$ ages. In this study, the discordances were calculated as [1-{(Age $^{206}Pb/^{238}U$)/(Age $^{207}Pb/^{235}U$)}] x 100 for zircons younger than 1.0 Ga and as [1-{(Age $^{206}Pb/^{238}U$)/(Age $^{207}Pb/^{206}Pb$)}] x 100 for zircons older than 1.0 Ga. A 10% discordance filter was used to visualize and compare the detrital age spectra.

DESCRIPTION OF ROCK AND ZIRCON SAMPLES

MICA SCHIST SM48/1

Mica schist sample SM48/1 was collected from an exposure exhibiting the characteristic lithology of the SMB upper unit, located ~600 m south-east of the Špičák Mt. (the Złote/Rychlebské Mts., 50°17'36"N, 17°1'23"E). In the lower part of the exposure studied, massive felsic metavolcanic rocks are in contact with garnet mica schists, and the latter are intercalated with a few to several centimeters of planar bodies of more massive finer-grained felsic metavolcanic rocks (Fig. 2A). The mica schists are several metres thick and disappear in favour of calcite marbles that are located in the upper part of the exposure. Sample SM48/1, which was collected from the central part of the exposure, consists of well-foliated, medium-grained mica schists. The schistosity is defined by a preferred orientation of muscovite and biotite flakes, and discontinuous, up to 1.2 mm-thick, quartz laminae. Sample SM48/1 also contains anhedral plagioclase and garnet porphyroblasts (up to 2 mm in diameter). Garnet and plagioclase grains contain inclusions of biotite, muscovite and quartz, all usually oriented obliquely to the main schistosity.

Most of the zircon grains studied in this sample are euhedral and subhedral (60%), whereas 40% are well or very well rounded (according to the nomenclature of Gärtner et al., 2013; Fig. 3A). They vary in length from ~90 to 220 μm. In contrast to sample SM9/2, sample SM48/1 contains more short prismatic crystals (67%), while those with elongations greater than 2.0 comprise the minority (43%). In transmitted light, the zircon grains are mostly transparent, colourless or orange (Fig. 4). Well-developed pyramids {101} are distinctive for this sample and dominate over {211}, while most of the grains have better developed {110} than {100} prisms (Fig. 3A). The most characteristic subtypes for these rocks are G1 and P1 (Fig. 3A).

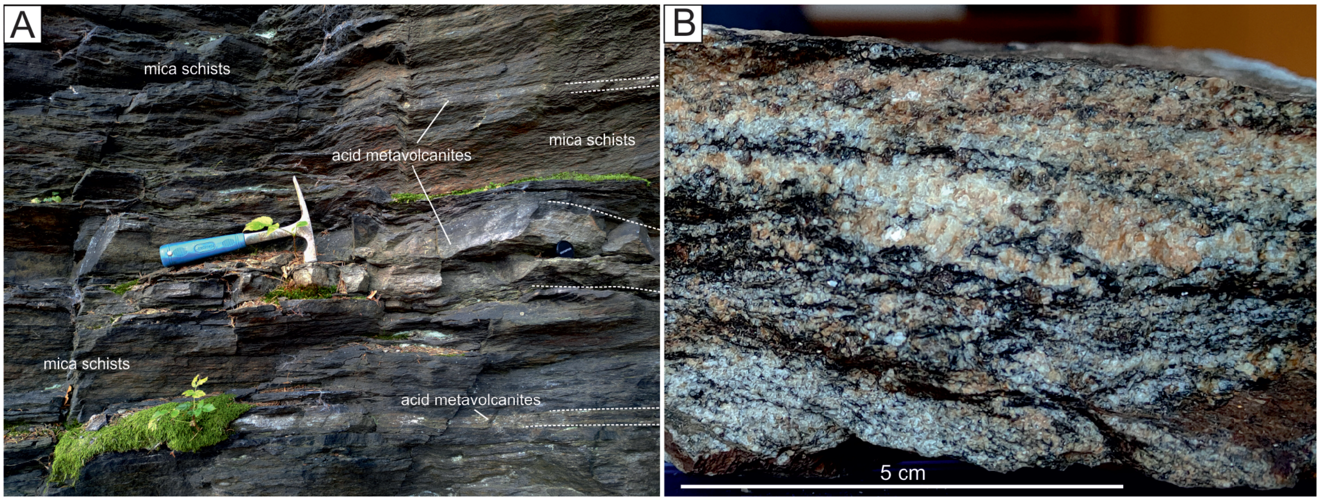

Fig. 2A – field photograph of mica schists (sample SM48/1) with intercalations of felsic metavolcanic rocks of the SMB upper unit; B – migmatized paragneiss of the SMB middle unit (sample SM9/2) with medium-grained leucocratic segregations

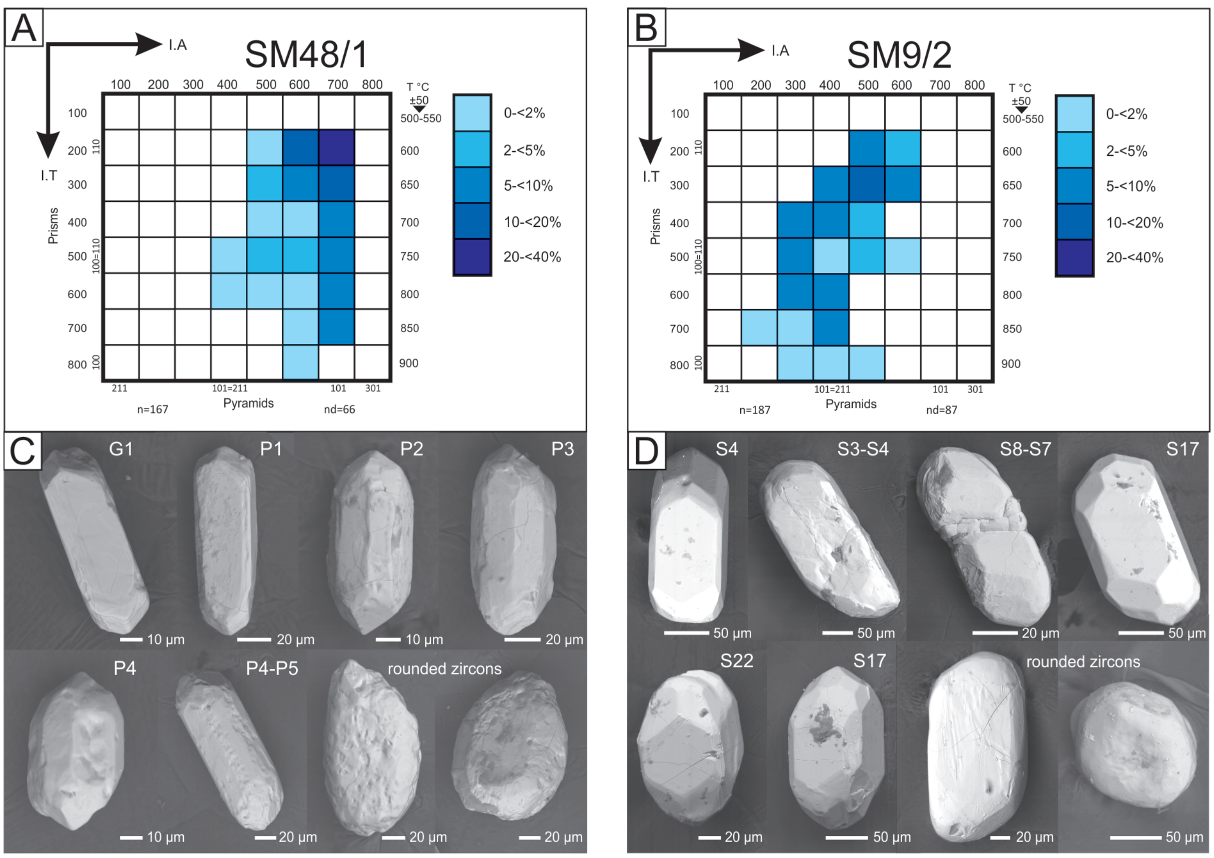

Fig. 3. Typological diagrams of zircon morphologies (according to Pupin, 1980) and secondary electron images (SEM) of representative zircon crystals

A – zircon populations of the SM48/1 mica schist: n – number of zircon crystals studied, nd – number of unclassified zircon crystals; **B** – zircon populations of the SM9/2 migmatitic paragneiss; **C** – SEM images of zircons from the mica schist (SM48/1); **D** – SEM images of zircons from the migmatitic paragneiss (SM9/2)

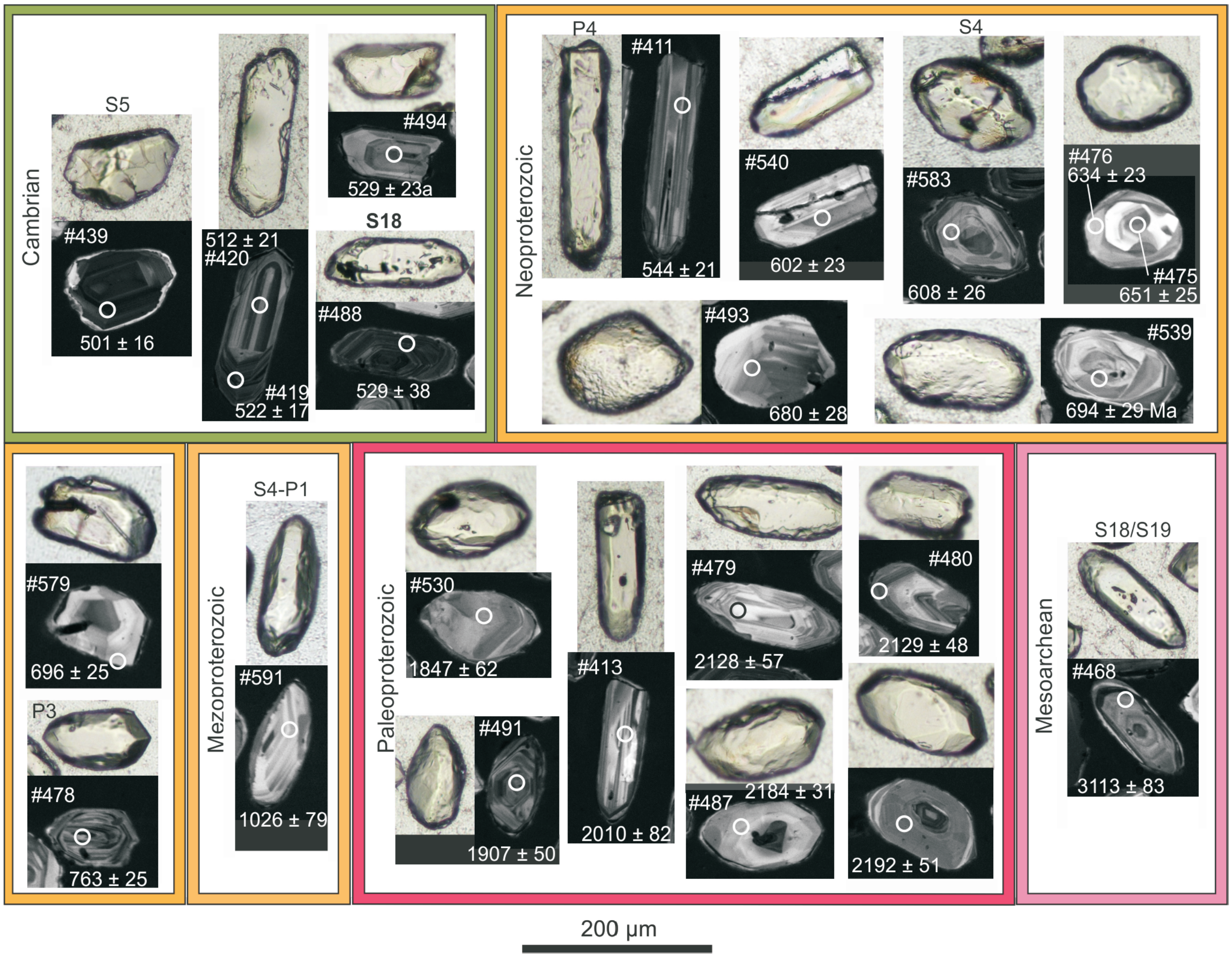

Fig. 4. Optical (upper or left) and cathodoluminescence images of zircons with ages (Ma) of representative crystals from sample SM48/1 (the upper unit)

MIGMATITIC PARAGNEISS SM9/2

Sample SM9/2 represents a high-grade paragneiss that is characteristic of the middle unit of the SMB. It was collected from an exposure located 1.5 km west of Stolec Mt. (Śnieżnik Massif) (50°12’37"N 16°57’19"E). In the exposure studied, migmatitic paragneisses predominate, with only one 15–20 cm-thick intercalation of felsic metavolcanic rock visible in its upper part. The migmatitic paragneiss SM9/2 is a weakly foliated rock that mainly consists of biotite, quartz, garnet, plagioclase and sillimanite that form a dark-coloured groundmass, and quartz and feldspars that concentrate in light-coloured migmatitic segregations. The dark-coloured groundmass is mostly fine-grained, although garnet grains form anhedral irregular blasts up to 2 mm in diameter, and plagioclase and quartz form occasional grains that are ~1 mm in diameter. Quartzo-feldspathic segregations (>1 cm-thick) are generally parallel to the main metamorphic foliation that is better developed in the darker, mica-rich groundmass. Quartzo-feldspathic segregations are coarser-grained, contain tabular, randomly oriented plagioclase grains that are 1 to 4 mm in diameter, interstitial quartz, anhedral garnet (2 mm in diameter) and subordinate biotite and chlorite. (Fig. 2B).

The zircons extracted from sample SM9/2 are well and very well rounded in 47% of the grains. Despite the mainly detrital origin of this rock, the other crystals (53%) are less rounded and include euhedral or subhedral grains that were suitable for Pupin’s (1980) classification. The grains are 80–250 µm in size, and their elongations (e.g., length/width aspect ratios) are mostly 2 to 3, with a few percent falling below and above these values. The morphological analysis shows a predominance of {110} prisms and well-developed {211} pyramids (Fig. 3B). In transmitted light, the crystals are transparent, mainly colourless or yellowish, and a small percentage of them contain inclusions (11%; Fig. 5). The predominant morphological subtypes are S4 and L4 (Fig. 3B).

NEW U-Pb ZIRCON DATA

The results of the LA-ICP-MS zircon dating of samples SM48/1 and SM9/2 are provided in the Appendix (Table S2) in the online supplement and are shown in Figure 6.

MICA SCHIST SM48/1

In sample SM48/1, U-Pb isotopic data were obtained from 138 analytical spots. A total of 125 analyses in 122 zircon crystals yielded concordant ages (Appendix, Table S2 and Fig. 6A). The oldest zircons or zircon cores (n = 3) are Archean in age

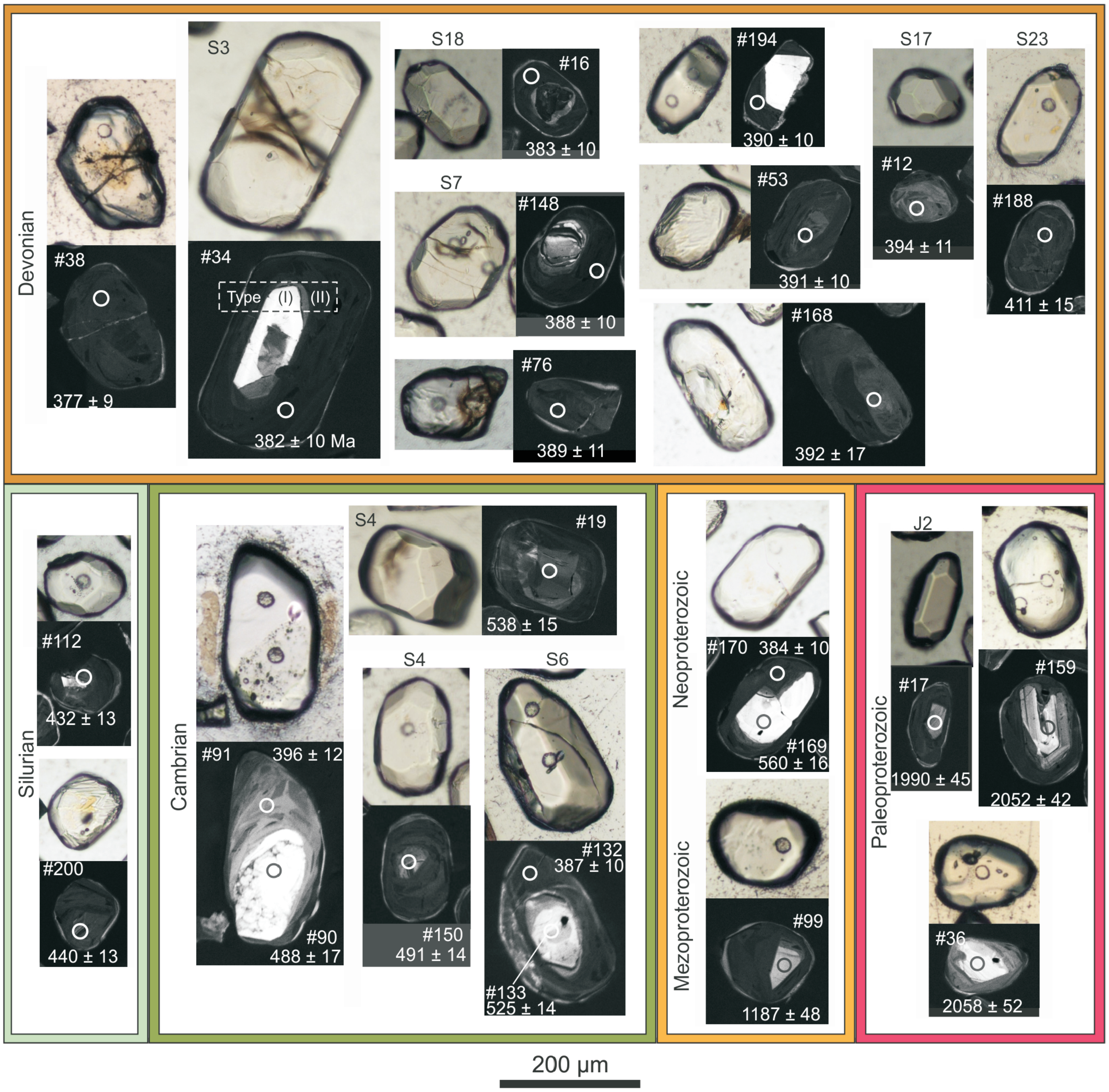

Fig 5. Optical (upper or left) and cathodoluminescence images of zircons with ages (Ma) of representative crystals from sample SM9/2 (the middle unit)

and yield ages of ~3.1 to ~2.7 Ga. One of these exhibits oscillatory zoning (#468, Fig. 4), and a second zircon exhibits a sector zoning pattern (#431 Appendix, Table S2). The third Archean age was obtained from a dark in CL, rounded core, which is mantled by a Neoproterozoic rim (#452, #453 Appendix, Table S2). Their Th/U ratios range from 1.02 to 1.49 (Fig. 7). The second most numerous population in this sample (n = 26) belongs to a Paleoproterozoic age cluster (2.46 to 1.85 Ga, Th/U = 0.39–0.65). Oscillatory zoning is the most common zircon texture in this group; however, sector zoning and zircons with inherited cores are also noticeable (Fig. 4). The transition between the Neoproterozoic and Mesoproterozoic is represented by two zircons that yielded ages of 1.03 and 0.99 Ga with Th/U ratios of 2.99 and 1.77, respectively (Fig. 7).

The largest zircon population is Neoproterozoic to Late Cambrian ranging between ~792 and 497 Ma (Fig. 6B). The main mode of this population is at ~605 Ma, while two other smaller maxima at ~653 Ma and 518 Ma are also evident (Fig. 6C). The zircons of this age are characterized by sector- or oscillatory-zoned textures and occasionally contain cores displaying different CL-induced luminescence (Fig. 4). Within this zircon population, the zircon cores yield ages that are often comparable to those obtained from their rims (Appendix, Table S2 and Fig. 4). The Th/U ratios for the zircons of this group range between 0.15 and 3.04; however, for most of the crystals, they are moderate and range between 0.37 and 2.06 (Fig. 7). A correlation between the roundness of the crystals and their ages can be observed. While the Cambrian grains have more elongated, euhedral forms, the older crystals are mostly subhedral or rounded (Appendix, Table S2 and Fig. 4).

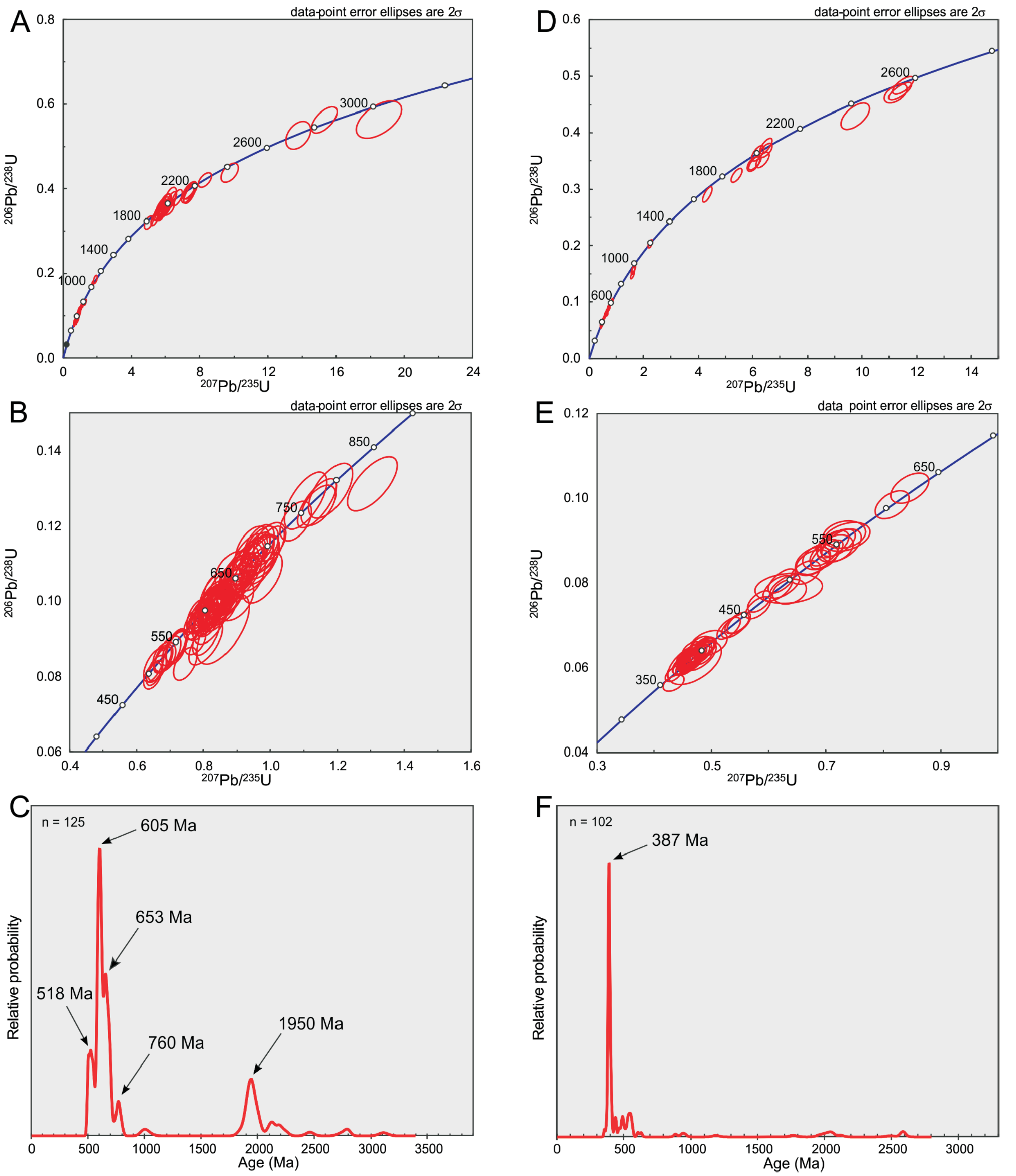

Fig. 6. U-Pb plots showing the zircon dating results

Only concordant or nearly concordant (10% discordant) analyses are shown; **A** – Wetherill diagram of zircon data from the upper unit sample – mica schist SM48/1; **B** – Wetherill diagram in the Neoproterozoic–Early Paleozoic range (sample SM48/1); **C** – probability density plot (sample SM48/1); **D** – Wetherill diagram of zircon data from the middle unit sample – mica schist SM9/2; **E** – Wetherill diagram in the Neoproterozoic–Early Paleozoic range (sample SM9/2); **F** – probability density plot (sample SM9/2)

Fig. 7. U-Pb ages vs. Th/U ratios for zircons from the metasedimentary rocks of the upper and middle units (this study) and the lower unit (Jastrzębski et al., 2015)

MIGMATITIC PARAGNEISS SM9/2

In sample SM9/2, 136 analyses in 87 zircon crystals were made. A total of 102 analyses were concordant within ±10% (Appendix, Table S2 and Fig. 6D). Based on the internal textures revealed by cathodoluminescence, two general types of zircon domain were distinguished. Type I zircon domains are cores that are either homogeneous or oscillatory zoned. Type II zircons or zircon domains predominate and form either whole zircon grains or zircon mantles that exhibit very low CL luminescence, which are surrounded by additional bright and very thin margins, while the latter are too narrow for isotopic analysis (Fig. 5). The mantles representing type II in individual cases can occasionally be thin and barely visible, but in most cases, they compose more than one-third of the area of the observed sections of the zircon grains.

In the more luminescent/oscillatory zoned grains or zircon cores (type I), four Neoarchean ages were obtained (2.50–2.59 Ga; Th/U = 0.22–0.73). Within the Proterozoic range (n = 20), seven zircon ages range from 2.12 to 1.96 Ga, one is 1.77 Ga, another is 1.18 Ga (Mesoproterozoic) and three ages are close to the Mesoproterozoic-Neoproterozoic transition, i.e., a range between 954 and 883 Ma (Fig. 6B). The rest (n = 8) of the oldest, type I zircon domains are Neoproterozoic and yield ~629–545 Ma ages. The Th/U ratios are within the range from 0.14 to 1.41 (Fig. 7); however, one crystal has a higher value of 2.36 (zircon #49, Appendix, Table S2 and Fig. 7). The youngest of the more luminescent zircon domains are late Cambrian in age (zircon #90, Fig. 5).

The type II zircon domains yield concordant Cambrian to Early Carboniferous ages (Figs. 5 and 6E). They are characterized by stable and low Th/U ratios that range between 0.20 and 0.33 for the Ordovician zircon ages and between 0.14 and 0.35 for the Silurian zircon ages (Appendix, Table S2, Figs. 5 and 7). The majority of the concordant ages that were obtained from the type II zircons in this sample are Devonian in age (n = 60) with a peak ~387 Ma (Fig. 6F). They have the lowest observed Th/U ratios (0.01–0.02; Fig. 7).

DISCUSSION

This study provides new zircon data from metasedimentary rocks that may help to unravel the age relationship between the protoliths of the metasedimentary and metavolcanic rocks of the SMB, with the latter dated as Cambrian to earliest Ordovician (Kröner et al., 2000; Jastrzębski et al., 2015). A primary observation of this work is that the metasedimentary rocks that represent the upper and middle lithotectonic units of the belt contain some important differences in their zircon age spectra (Fig. 7). The zircon age spectra obtained from sample SM48/1 (the upper unit, “Hranična” mica schists) are dominated by Neoproterozoic and Paleoproterozoic age clusters, which are comparable to those obtained from the Brusek quartzites from the lower unit of the SMB (Jastrzębski et al., 2015; Fig. 7). Nevertheless, the Brusek quartzites contain very rounded zircon grains, which contrast with the results of the morphological zircon study of the upper unit sample, SM48/1, which revealed various shapes, including euhedral zircons (Fig. 3A, C). This suggests less prolonged sedimentary transport of the detrital material contained in the sample from the upper unit. The other main difference is that the sample from the upper unit contains Late Cambrian zircon ages that are absent from the Brusek quartzites. The zircon grains of this age are generally more euhedral than the other, Neoproterozoic and older grains (Fig. 4

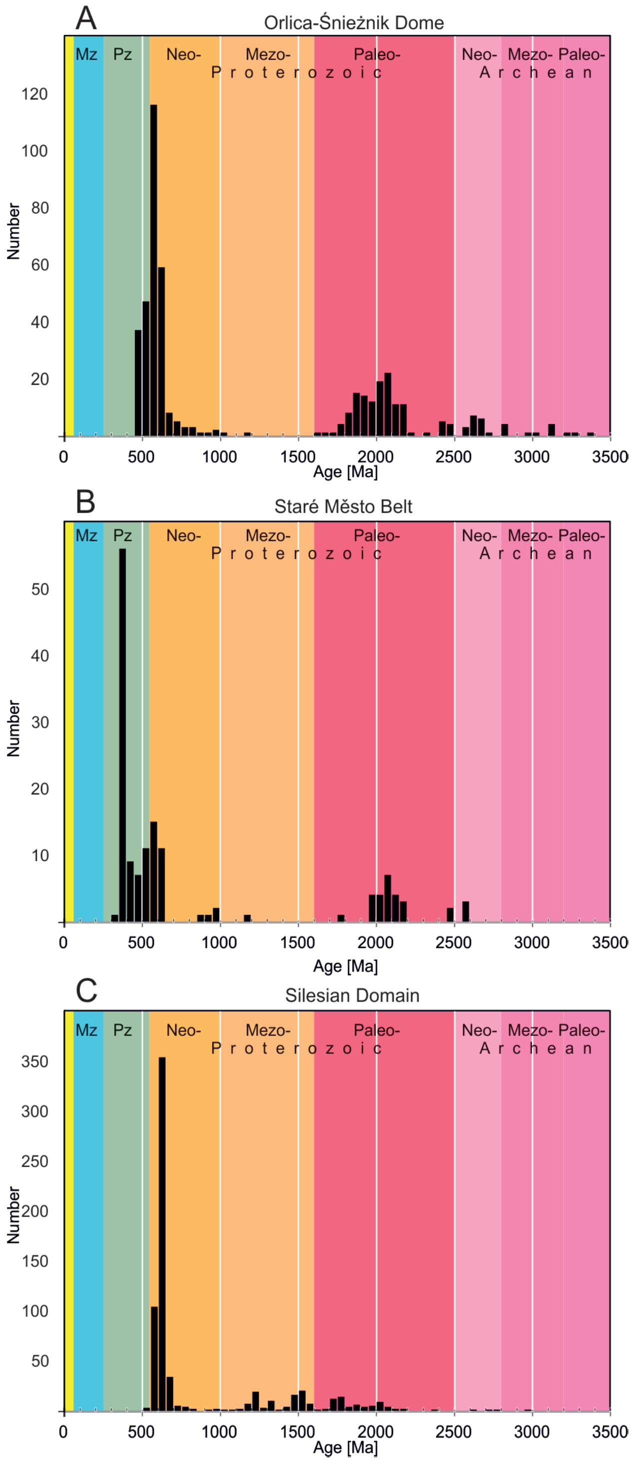

Fig. 8. Comparison of detrital age spectra of the units in the Central Sudetes

A – detrital zircon age spectra of the metasedimentary rocks of the Orlica–Śnieżnik Dome compiled from Jastrzębski et al. (2010), Mazur et al. (2012, 2015) and Szczepański et al. (2020); **B** – detrital zircon age spectra of the Staré Město Belt (Jastrzębski et al., 2015, this study); **C** – detrital zircon age spectra of the Velké Vrbno, Keprník and Desná domes (Jastrzębski et al., 2021); in the histograms, analyses with <10% discordance are shown; Pz – Paleozoic, Mz – Mesozoic

and Appendix, Table S2), so they can be interpreted either as detrital grains that underwent very short sedimentary transport or grains that were directly supplied by concurrent volcanic activity. Our field observations and geological mapping results indicate that the felsic metavolcanic rocks formed recurrent and variously thick (from 1 cm to ~200 m thick) intercalations within the metapelites of the SMB upper unit (Fig. 2A; e.g., Don et al., 2003). Such an arrangement consisting of alternating thin metavolcanic and metapelitic rocks may be difficult to interpret in terms of the Variscan tectonism and juxtaposition of volcanic and pelitic rocks. A primary mutual relationship and the same protolith age of the felsic metavolcanic rocks and metapelites as a part of the same volcano-sedimentary sequence are more probable. The protolith ages of the accompanying felsic metavolcanic rocks are Early Cambrian (Kroner et al., 2000) or Late Cambrian (Jastrzębski et al., 2015). In this interpretation, the Late Cambrian zircons are best interpreted as a volcanic admixture to the mainly pelitic volcano-sedimentary succession of the SMB upper unit.

On the other hand, the migmatitic paragneiss, SM9/2, in the middle unit contains a large number of Ordovician to Early Carboniferous zircon ages, which fall along the concordia line (Fig. 6E) and are absent from the age spectra of sample SM48/1. A scatter of zircon ages along the concordia line was obtained in this region in high-grade eclogites and granulites of the Orlica-Śnieżnik Dome and was interpreted as age resetting due to the Variscan overprint (Bröcker et al., 2010; Walczak et al., 2017). In sample SM9/2, these zircon ages were obtained from type II zircons. A weak correlation between the Th/U ratios and apparent ages among the type II zircons indicates that the Th/U ratios are lower in younger grains (Fig. 7). Solid-state recrystallization under high-grade metamorphic conditions can produce both the observed correlations of the apparent ages and Th/U ratios and result in U-Pb dates that are younger than the crystallization ages (see Hoskin and Black, 2000). It is thus suggested that the type II zircon domains in sample SM9/2 are the result of metamorphic transformation of Cambrian and older zircon grains rather than new zircon growth. The isotopic composition and texture of the pre-existing zircons were presumably disturbed by diffusion reaction processes under high-grade conditions. This interpretation is in line with earlier studies of the behaviour of zircon in partial melting conditions that were conducted in the southern part of the Bohemian Massif (Siebel et al., 2012) and in the central part of the massif (Žák et al., 2017). It is still possible that the zircon rims, especially the very thin brighter cathodoluminescence zones at their margins that are commonly observed in this sample, and the well-developed prisms visible in transmitted light, can reflect new zircon growth (Fig. 5). The zircon typological analysis of this sample indicates large numbers of euhedral grains that show a predominance of well-developed {211} pyramids and {110} prisms with the majority of morphotypes being type S4, which can refer to the development of very thin zircon rims. The greatest number of zircon morphotypes that belong to types S4, S3 or S2 (Figs. 3B and 5) may be an indicator of migmatization according to Pupin (1980). A significant number of discordant ages in sample SM9/2 compared to that observed for sample SM48/1 (Appendix, Table S2) suggests a partial Pb-loss in SM9/2 zircons and advocates for disturbance of zircon structure in the high-grade middle unit.

The accompanying Late Cambrian amphibolites of the middle unit underwent temperature conditions that exceeded 700°C (Bartz, 2004; Lexa et al., 2005). Our data obtained from the low-luminescence domains of sample SM9/2 (type II zircons) might suggest that the metamorphic transformations of the zircon structure climaxed at ~387 Ma. This age maximum is older than the garnet and monazite ages of the SMB, the latter showing that the metamorphism in the belt took place from ~368 to 335 Ma (Jastrzębski et al., 2013). Nevertheless, our new data might support the Early Variscan (Devonian) metamorphism along the western margin of the Brunovistulia that was recently documented by Sorger et al. (2020) in Lower Austria. In conclusion, the youngest zircon ages of this sample do not refer to the depositional age or maximum depositional age of the metasedimentary rocks of the middle unit but to Early Variscan metamorphic transformations. The youngest ages that were obtained from the type I zircon domains are Cambrian in age, which do not contradict the interpretation that the paragneisses of the middle unit are part of a volcano-sedimentary sequence in which Late Cambrian metaigneous rocks dominated.

The new age data obtained from the zircons that were not affected by metamorphic transformations also contribute to the questions regarding the provenances and terrane affiliations of the separate lithotectonic units of the SMB. The detrital zircon age spectra from the upper unit of the SMB refer to those of the Orlica-Śnieżnik Dome (see Jastrzębski et al., 2010; Mazur et al., 2012, 2015; and Szczepański et al., 2020; Fig. 8), and the other spectra are known to be from the Saxothuringian terrane (e.g., Linnemann et al., 2004; Oberc-Dziedzic et al., 2018 for review). Fewer pre-Variscan age data were obtained from the middle unit paragneisses; nevertheless, when excluding the age data from the type II zircons, the predominance of Neoproterozoic and Paleoproterozoic zircon ages and the presence of Cambrian zircon ages are also evident. The source area for the sedimentary basin of the SMB middle unit is thus unlikely to be the adjacent Velké Vrbno Dome (the Brunovistulian microplate), the zircon age spectra of which lack Cambrian ages and contain a significant population of 1.7–1.2 Ga zircon ages (Jastrzębski et al., 2021; Fig. 8). The zircon age pattern obtained is thus more comparable to that obtained for the metasedimentary rocks of the Orlica–Śnieżnik Dome (Fig. 8), and consequently, the source areas of the sedimentary basins of both the upper, middle and lower units of the belt can likely be linked to the West African Craton, which was once located in northern Gondwana, from which the Saxothuringian terrane was derived (e.g., Linnemann et al., 2004; Stephan et al., 2018). The African provenance of the eastern margin of the Saxothuringian terrane (Jastrzębski et al. 2015; this study) and the presumed Amazonian provenance of the Sudetic portions of the Brunovistulian terrane (Jastrzębski et al., 2021) may support the notion of an ocean separating the two terranes before their Variscan amalgamation (e.g., Finger and Steyrer, 1995). Our data indicate that all the three subunits of the SMB are best correlated with the Saxothuringian terrane, that the Variscan metamorphic evolution of the SMB started in the Devonian, and that the main Variscan suture in this region is located along the eastern margin of the SMB.

CONCLUSIONS

1. The new detrital zircon age spectra of the metasedimentary rocks of the upper and middle units of the Staré Město Belt, when compared to previously published zircon age data from the metavolcanic rocks of the belt, suggest that metasedimentary and bimodal metavolcanic rocks originally formed Late Cambrian volcano-sedimentary successions. In the upper unit of the SMB, pelitic sedimentation dominated over felsic volcanic effusion, while in the middle unit, the succession was dominated by bimodal volcanic rocks.

2. The source areas of the sedimentary basins studied were dominated by Neoproterozoic and Paleoproterozoic crystalline rocks that were presumably located near the West African Craton of Gondwana. The present and previously published data consequently suggest that the entire SMB is a part of the Saxothuringian terrane and its eastern termination formed in the Sudetes.

3. A partial melting event under high-grade metamorphic conditions during Variscan consolidation, characteristic of the middle unit of the SMB, was responsible for a solid-state transformation of Cambrian and older zircon grains in the Devonian. It produced partial resetting of the U-Pb dates, changes in internal zircon textures and reductions in Th/U ratios.

Acknowledgments. This study was financed by NCN grants 2018/29/B/ST10/01120 and 2014/15/B/ST10/03938. J. Sláma was supported by the CAS support RVO 67985831. A. Jaźwa, I. Kocjan and J. Nowak of the technical staff of the Institute of Geological Sciences, Polish Academy of Sciences (ING PAN) are thanked for the preparation of thin sections and zircon grain separation. M. Prell from the Institute of Geological Sciences of University of Wrocław is thanked for her assistance with SEM imaging. We appreciate the constructive and detailed reviews provided by F. Finger and B. Bagiński. We also thank L. Krzemiński for careful editorial handling.

REFERENCES

Aguilar, C., Štípská, P., Chopin, F., Schulmann, K., Pitra, P., Závada, P., Hasalová, P., Martelat, J., 2020. Syn-deformational melt percolation through a high-pressure orthogneiss and the exhumation of a subducted continental wedge (Orlica–Śnieżnik Dome, NE Bohemian Massif). International Journal of Earth Sciences, **109**: 1213–1246.

Aleksandrowski, P., Mazur, S., 2002. Collage tectonics in the northeasternmost part of the Variscan Belt: the Sudetes, Bohemian Massif. Geological Society Special Publications, **201**: 237–277.

Bartz, W., 2004. Metamorphic evolution of the amphibolites from the Polish part of Stare Město Zone (Sudetes, SW Poland). Mineralogia Polonica, **35**: 57–74.

Bederke, E., 1929. Die Grenze von Ost- und Westsudeten und ihre Bedeutung für die Einordnung der Sudeten in den Gebirgsbau Mitteleuropas (in German). Geologische Rundschau, **20**: 186–205.

Bröcker, M., Klemd, R., Kooijman, E., Berndt, J., Larionov, A., 2010. Zircon geochronology and trace element characteristics of eclogites and granulites from the Orlica–Śnieżnik complex, Bohemian Massif. Geological Magazine, **147:** 339–362.

Chopin, F., Schulmann, K., Skrzypek, E., Lehmann, J. Dujardin, J.R., Martelat, E., Lexa, O., Corsini, M., Edel, J.B., Štípská, P., Pitra, P., 2012. Crustal influx, indentation, ductile thinning and gravity redistribution in a continental wedge: building a Moldanubian mantled gneiss dome with underthrust Saxothuringian material (European Variscan belt). Tectonics, **31**, **TC1013.**

Cloos, H., 1922. Die Gebirgsbau Schlesien und die Stellung seiner Bodenschätze (in German). Verlag von Gebrüder Borntraeger, Berlin.

Collett, S., Štípská., P., Schulmann., K., Míková., J., Kröner., A., 2021. Tectonic significance of the Variscan suture between Brunovistulia and the Bohemian Massif. Journal of the Geological Society, **178**. jgs2020-176.

Cymerman, Z., 1993. Does the Ramzova Thrust exist in the Sudetes? (in Polish with English summary). Przegląd Geologiczny, **41**: 700–706.

Cymerman, Z., Piasecki, M.A.J., Seston, R., 1997. Terranes and terrane boundaries in the Sudetes, Northeast Bohemian Massif. Geological Magazine, **134**: 717–725.

Don, J., Skácel, J., Gotowała, R., 2003. The boundary zone of the East and West Sudetes on the 1:50,000 scale geological map of the Velké Vrbno, Staré Město and Śnieżnik Metamorphic Units. Geologia Sudetica, **35**: 25–59.

Finger, F., Steyrer, H.P., 1995. A tectonic model for the eastern Variscides: indications from a chemical study of amphibolites in the south-eastern Bohemian Massif. Geologica Carpathica, **46**: 137–150.

Floyd, P.A., Winchester, J.A., Ciesielczuk, J., Lewandowska, A., Szczepański, J., Turniak, K., 1996. Geochemistry of early Palaeozoic amphibolites from the Orlica–Śnieżnik Dome, Bohemian Massif: petrogenesis and palaeotectonic aspects. Geologische Rundschau, **85**: 225–238.

Floyd, P.A., Winchester, J.A., Seston, R., Kryza, R., Crowley, Q.G., 2000. Review of geochemical variation in Lower Palaeozoic metabasites from the NE Bohemian Massif: intracratonic rifting and plume–ridge interaction. Geological Society Special Publications, **179**: 155–174.

Franke, W., Żelaźniewicz, A., 2000. The eastern termination of the Variscides: terrane correlation and kinematic evolution. Geological Society Special Publications, **179**: 63–86.

Gärtner, A., Linnemann, U., Sagawe, A., Hofmann, M., 2013. Morphology of zircon crystal grains in sediments – characteristics, classifications, definitions. Geologica Saxonica, **59**: 65–73.

Gawlikowska, E., Opletal, M., 1997. Králický Sněžník – geologicka mapa pro turisty (Śnieżnik Area – Geological Map for Tourists). Český geologický ústav, Państwowy Instytut Geologiczny.

Hoskin, P.W.O., Black, L.P., 2000. Metamorphic zircon formation by solid-state recrystallization of protolith igneous zircon. Journal of Metamorphic Geology, **18**: 423–439.

Jastrzębski, M., 2012. New insights into the polyphase evolution of the Variscan suture zone: evidence from the Staré Město Belt, NE Bohemian Massif. Geological Magazine, **149**: 945–963.

Jastrzębski, M., Żelaźniewicz, A., Nowak, I., Murtezi, M., Larionov, A.N., 2010. Protolith age and provenance of metasedimentary rocks in Variscan allochthon units: U-Pb SHRIMP zircon data from the Orlica–Śnieżnik Dome, West Sudetes. Geological Magazine, **147**: 416–433.

Jastrzębski, M., Żelazniewicz, A., Majka, J., Murtezi, M., Bazarnik, J., Kapitonov, I., 2013. Constraints on the Devonian–Carboniferous closure of the Rheic Ocean from a multi-method geochronology study of the Staré Město Belt in the Sudetes (Poland and the Czech Republic). Lithos, **170–171**: 54–72.

Jastrzębski, M., Żelaźniewicz, A., Murtezi, M., Larionov, A.N., Sergeev, S., 2015. The Moldanubian Thrust Zone – a terrane boundary in the Central European Variscides refined based on lithostratigraphy and U-Pb zircon geochronology. Lithos, **220–223**: 116–132.

Jastrzębski, M., Machowiak, K., Krzemińska, E., Farmer, L.G., Larionov, A.N., Murtezi, M., Majka, J., Sergeev, S., Ripley, E.M., Whitehouse, M., 2018. Geochronology, petrogenesis and geodynamic significance of the Visean igneous rocks in the Central Sudetes, northeastern Bohemian Massif. Lithos, **316–317**: 385–405.

Jastrzębski, M., Żelaźniewcz, A., Sláma, J., Machowiak, K., Śliwiński, M., Jaźwa, A., Kocjan, I., 2021. Provenance of Precambrian basement of the Brunovistulian Terrane: new data from its Silesian part (Czech Republic, Poland), central Europe, and implications for Gondwana break-up. Precambrian Research, **355**: article 106108.

Kröner, A., Štipská, P., Schulmann, K., Jaeckel, P., 2000. Chronological constraints on the pre-Variscan evolution of the northeastern margin of the Bohemian Massif, Czech Republic. Geological Society Special Publications, **179**: 175–197.

Lexa, O., Štípská, P., Schulmann, K., Baratoux, L., Kröner, A., 2005. Contrasting textural record of two distinct metamorphic events of similar P–T conditions and different durations. Journal of Metamorphic Geology, **23**: 649–666.

Linnemann, U., McNaughton, N.J., Romer, R.L., Gehmlich, M., Drost, K., Tonk, C., 2004. West African provenance for Saxo-Thuringia (Bohemian Massif): did Armorica ever leave pre-Pangean Gondwana? International Journal of Earth Sciences, **93**: 683–705.

Matte, P., Maluski, H., Rajlich, P., Franke, W., 1990. Terrane boundaries in the Bohemian Massif: result of large-scale Variscan shearing. Tectonophysics, **177**: 151–170.

Mazur, S., Aleksandrowski, P., Kryza, R., Oberc-Dziedzic, T., 2006. The Variscan orogen in Poland. Geological Quarterly, **50** (1): 89–118.

Mazur, S., Szczepański, J., Turniak, K., McNaughton, N.J., 2012. Location of the Rheic suture in the eastern Bohemian Massif: evidence from detrital zircon data. Terra Nova, **24**: 199–206.

Mazur, S., Turniak, L., Szczepański, J., McNaughton, N.J., 2015. Vestiges of Saxothuringian crust in the Central Sudetes, Bohemian Massif: zircon evidence of a recycled subducted slab provenance. Gondwana Research, **27**: 825–839.

Oberc, J., 1968. The boundary between the western and eastern Sudetic tectonic structures (in Polish with English summary). Rocznik Polskiego Towarzystwa Geologicznego, **38**: 203–217.

Oberc-Dziedzic, T., Kryza, R., Pin, C., 2015. Variscan granitoids related to shear zones and faults: examples from the Central Sudetes (Bohemian Massif) and the Middle Odra Fault Zone. International Journal of Earth Sciences, **104:** 1139–1166.

Oberc-Dziedzic, T., Kryza, R., Madej, S., Pin, C., 2018. The Saxothuringian Terrane affinity of the metamorphic Stachów Complex (Strzelin Massif, Fore-Sudetic Block, Poland) inferred from zircon ages. Geological Quarterly, **62** (2): 237–256.

Oberc-Dziedzic, T., Pin, C., Madej, S., Kryza R., 2021. Reconstruction of the thermal history of the northwestern part of the Brunovistulicum. International Journal of Earth Sciences, **110**: 2091–2114.

Opletal, M., Pecina, V., 2004. The Ramzova tectonic zone: the contact between Lugicum and Silesicum. Acta Geodynamica et Geomaterialia, **1**: 41–47.

Parry, M., Štípská, P., Schulmann, K., Hrouda, F., Ježek, J., Kröner, A., 1997. Tonalite sill emplacement at an oblique boundary: northeastern margin of the Bohemian Massif. Tectonophysics, **280**: 61–81.

Poubová, E., Sokol, A., 1992. The petrology and geochemistry of themetaophiolitic rocks of Stare Město crystalline unit. Krystalinikum, **21**: 67–88.

Pupin, J.P., 1980. Zircon and granite petrology. Contributions to Mineralogy and Petrology, **73**: 207–220.

Schulmann, K., Gayer, R., 2000. A model of an obliquely developed continental accretionary wedge: NE Bohemian Massif. Journal of the Geological Society, **156**: 401–416.

Siebel, W., Shang, C.K., Thern, E., Danisik, M., Rohrmueller, J., 2012. Zircon response to high-grade metamorphism as revealed by U-Pb and cathodoluminescence studies. International Journal of Earth Sciences, **101**: 2105–2123.

Skácel, J., 1977. The character of contacts between the Snieżnik gneisses and the Stare Miasto crystalline rocks (in Polish with

English summary). Acta Universitatis Wratislaviensis, **378**: 207–215.

Skácel, J., 1989. On the Lugicum – Silesicum boundary (in Czech with English summary). Prace Geologiczno-Mineralogiczne, Acta Universitatis Wratislaviensis, **17**: 45–55.

Sorger, D., Hauzenberger, C.A., Finger, F., Linner, M., 2020. Two generations of Variscan garnet: implications from a petrochronological study of a high grade Avalonia-derived paragneiss from the Drosendorf unit, Bohemian Massif. Gondwana Research, **85**: 234–148.

Stephan, T., Kroner, U., Romer, R.L., 2019. The pre-orogenic detrital zircon record of the Peri-Gondwanan crust. Geological Magazine, **156:** 281–307.

Štípská, P., Schulmann, K., Thompson, A.B., Ježek, J., Kröner, A., 2001. Thermo-mechanical role of a Cambro-Ordovician paleorift during the Variscan collision: the NE margin of the Bohemian Massif. Tectonophysics, **332**: 239–253.

Štípská, P., Schulmann, K., Kröner, A., 2004. Vertical extrusion and middle crust spreading of omphacite granulite: a model of syn-convergent exhumation (Bohemian Massif, Czech Republic). Journal of Metamorphic Geology, **22**: 179–198.

Štípská, P., Pitra, P., Powell, R., 2006. Separate or shared metamorphic histories of eclogites and surrounding rocks? An example from the Bohemian Massif. Journal of Metamorphic Geology, **24**: 219–240.

Szczepański, J., Turniak, K., Anczkiewicz, R., Gleichner, P., 2020. Dating of detrital zircons and tracing the provenance of quartzites from the Bystrzyckie Mts: implications for the tectonic setting of the Early Palaeozoic sedimentary basin developed on the Gondwana margin. International Journal of Earth Sciences, **109**: 2049–2079.

Walczak, K., Anczkiewicz, R., Szczepański, J., Rubatto, D., Košler, J., 2017. Combined garnet and zircon geochronology of the ultra-high temperature metamorphism: constraints on the rise of the Orlica–Śnieżnik Dome, NE Bohemian Massif, SW Poland. Lithos, **292–293**: 388–400.

Wierzchołowski, B., 1966. Bielice granitoids in the Sudetes and their country rocks (in Polish with English summary). Archiwum Mineralogiczne, **26**: 509–647.

Žák, J., Sláma, J., Burjak, M., 2017. Rapid extensional unroofing of a granite-migmatite dome with relics of high-pressure rocks, the Podolsko complex, Bohemian Massif. Geological Magazine, **154**: 354–380.

APPENDIX

LA-ICP–MS U-(Th-)Pb analytical data and results of zircon dating of samples SM48/1 and SM8/2

Table S1
LA-ICP-MS U-(Th-)Pb analytical data
(reporting template according to Horstwood et al., 2016)

Laboratory and sample preparation	
Laboratory name	Institute of Geology of the Czech Academy of Sciences, Prague, Czech Republic
Sample type/mineral	zircon
Sample preparation	Conventional mineral separation, 1 inch resin mount
Imaging	CL, JEOL JXA-8530F Field Emission EPMA, Institute of Petrology and Structural Geology, Charles University in Prague
Laser ablation system	
Make, model and type	Teledyne Cetac Analyte Excite laser
Ablation cell and volume	built-in 2-volume cell HelEx II, 100 x 100 mm
Laser wavelength (nm)	193 nm
Pulse width (ns)	<4 ns
Fluence (J cm^{-2})	3.5 J cm^{-2}
Repetition rate (Hz)	5 Hz
Ablation duration (s)	35 s
Spot diameter (mm)	25 mm
Sampling mode/pattern	Static spot ablation
Carrier gas	100% He + little addition N2 in the cell, Ar make-up gas combined using a Y-piece along the sample transport line to the torch. All gases and aerosole are mixed in the in-house glass signal homogenizer (design of Tunheng and Hirata, 2004) right before entering torch
Cell carrier gas flow (l min^{-1})	0.91 l min^{-1}
N2 flow (ml min^{-1})	4.9 ml min^{-1}
Ar make-up gas flow (l min^{-1})	0.68 l min^{-1}
ICP-MS instrument	
Make, model and type	Thermo Scientific double-focusing magnetic sector field Element 2 HR-ICP-MS
Sample introduction	Dry ablation aerosol
RF power (W)	1200 W
Detection system	discrete dynode, dual mode secondary electron multiplier (SEM); analysis possible in 3 modes (cps-analog-both)
Masses measured (mode)	204 (cps), 206 (both), 207 (cps), 208 (cps), 232 (both), 235 (cps), 238 (both)
Integration time per peak/dwell times (ms)	204 (10 ms), 206 (15 ms), 207 (30 ms), 208 (10 ms), 232 (10 ms), 235 (20 ms), 238 (10 ms)
Total integration time per output data point (s)	~0.12 s (time resolution of the data)
Data processing	
Initial calculation	The accuracy of 238 mass measured in "both" mode is dependent on the correctly determined ACF (Analog Correction Factor) In order to correct for this variability, the data are pre-processed using a Python routine for decoding the Thermo Element ICPMS dat files (Hartman et al., 2017) and an in-house Excel macro. As a result, the intensities of 238 are left unchanged if measured in a counting mode and recalculated from ^{235}U intensities (using the natural $^{138}U/^{135}U$ of 137.818) in all cases the ^{238}U was acquired in analog mode, thus eliminating the non-linearity between pulse counting and analog detecting modes.
Gas blank	15 s on-peak zero subtracted
Calibration strategy	Plešovice used as primary reference material, 91500 and GJ1 used as secondaries/validation
Reference material information, reference age	Plešovice (Sláma et al., 2008), 337 Ma (Concordia age)
	91500 (Wiedenbeck et al., 1995), 1065 Ma (Concordia age)
	GJ1 (Jackson et al., 2004), 609 Ma (206Pb/207Pb age)
Data processing package used/correction for LIEF	Iolite v3.5 software (Paton et al., 2010) with the VizualAge utility (Petrus and Kamber, 2012) used for data normalisation, uncertainty propagation and export
	blank intensities and instrumental bias interpolated using an automatic spline function; down-hole inter-element fractionation (LIEF) corrected using an exponential function
	LIEF correction assumes reference material and samples behave identically
	Isoplot v4_16 (Ludwig, 2008) used for pooled age uncertainty propagation, age calculation and plotting
Common-Pb correction, composition and uncertainty	No common-Pb correction applied to the data
Uncertainty level and propagation	Ages are quoted at 2s absolute, propagation is by quadratic addition
	Reproducibility and age uncertainty of reference material are propagated where appropriate following the recommendation of Horstwood et al. (2016)
Quality control/validation	91500 – Concordia age = 1057 ± 9 Ma (2s, MSWD = 0.9, n = 58)
	GJ-1 – Concordia age = 604 ± 5 (2s, MSWD = 1.2, n = 58)
	Systematic uncertainty for propagation is 2% (2s)
Other information	20 s wait time between ablations
References	Hartman, J., Franks, R., Gehrels, G., Hourigan, J., Wenig, P., 2017. Decoding data files from a Thermo ElementTM ICP Mass Spectrometer. Manual available online at https://github.com/jhh67/extractdat.git Horstwood, M.S.A., Košler, J., Gehrels, G., Jackson, S.E., McLean, N.M., Paton, C., Pearson, N.J., Sircombe, K., Sylvester, P., Vermeesch, P., Bowring, J.F., Condon, D.J. and Schoene, B., 2016. Community-Derived Standards for LA-ICP-MS U-(Th-)Pb Geochronology – Uncertainty Propagation, Age Interpretation and Data Reporting. Geostand. Geoanal. Res., **40**: 311–332.

Jackson, S.E., Pearson, N.J., Griffin, W.L., Belousova, E.A., 2004. The application of laser ablation-inductively coupled plasma-mass spectrometry to in situ U-Pb zircon geochronology. Chemical Geology, **211**: 47–69.
Ludwig, K.R., 2008. User's manual for Isoplot 3.70: a geochronological toolkit for Microsoft Excel. Berkeley Geochronological Center, Special Publication, **4**: 1–76.
Paton, C., Woodhead, J.D., Hellstrom, J.C., Hergt, J.M., Greig, A., Maas, R., 2010. Improved laser ablation U-Pb zircon geochronology through robust downhole fractionation correction. Geochemistry, Geophysics, Geosystems, **11**.
Petrus, J.A., Kamber, B.S., 2012. Vizual Age: a novel approach to laser ablation ICP-MS U-pb geochronology data reduction. Geostand. Geoanal. Res., **36**: 247–270.
Sláma, J., Kosler, J., Condon, D.J., Crowley, J.L., Gerdes, A., Hanchar, J.M., Horstwood, M.S.A., Morris, G.A., Nasdala, L., Norberg, N., Schaltegger, U., Schoene, B., Tubrett, M.N., Whitehouse, M.J., 2008. Plesovice zircon – a new natural reference material for U-Pb and Hf isotopic microanalysis. Chemical Geology, **249**: 1–35.
Tunheng, A., Hirata, T., 2004. Development of signal smoothing device for precise elemental analysis using laser ablation-ICP-mass spectrometry. Journal of Analytical Atomic Spectrometry, **19**: 932.
Wiedenbeck, M., Alle, P., Corfu, F., Griffin, W.L., Meier, M., Oberli, F., Vonquadt, A., Roddick, J.C., Speigel, W., 1995. 3 natural zircon standards for U-Th-Pb, Lu-Hf, trace-element and REE analyses. Geostandards Newsletter, **19**: 1–23.

Table S2
Results of LA-ICP-MS dating of zircons coming from metasedimentary rocks of the Staré Město Belt

Analyses with more than 10% of discordance are indicated by grey font, analyses indicated by red font refer to data obtained from zircons with euhedral shapes

Discordance was calculated as (1-((AGE $^{206}Pb/^{238}U$)/ (AGE $^{207}Pb/^{235}U$)))*100 for zircons younger than 1.0 Ga and as (1-((AGE $^{206}Pb/^{238}U$)/ (AGE $^{207}Pb/^{206}Pb$)))*100 for zircons older than 1.0 Ga

Spot		Concentartion (ppm)				Isotope ratio								Age (Ma) and discordance (%)						
		Pb	Th	U	Th/U	$^{206}Pb/^{204}Pb$	$^{207}Pb/^{235}U$	±2σ (abs)	$^{206}Pb/^{238}U$	±2σ (abs)	$^{207}Pb/^{206}Pb$	±2σ (abs)	Err.Corr.	$^{207}Pb/^{235}U$ age	±2σ (abs)	$^{206}Pb/^{238}U$ age	±2σ (abs)	$^{207}Pb/^{206}Pb$ age	±2σ (abs)	discordance
Sample SM48/1 – mica schists																				
1	#407	1422	555	553	1.004	910000	0.648	0.022	0.080	0.003	0.0587	0.0019	0.48138	503	13	497	17	523	71	1.2
2	#439	1316	530	294	1.802	420000	0.654	0.020	0.081	0.003	0.0588	0.0015	0.6158	506	12	501	16	509	56	1.0
3	#408	566	223	285	0.782	550000	0.654	0.020	0.081	0.002	0.0588	0.0014	0.57541	508	12	503	15	524	54	1.0
4	#550	489	188	309	0.609	86000	0.662	0.022	0.082	0.003	0.0594	0.0018	0.50068	512	13	509	17	530	66	0.6
5	#420	434	167	236	0.708	260000	0.652	0.025	0.083	0.004	0.0580	0.0018	0.60986	505	16	512	21	479	67	-1.4
6	#458	1437	482	661	0.729	230000	0.746	0.029	0.083	0.004	0.0667	0.0025	0.52039	561	17	514	22	779	80	8.4
7	#419	225	91	239	0.379	450000	0.678	0.021	0.085	0.003	0.0592	0.0016	0.59517	521	12	522	17	532	58	-0.2
8	#582	368	133	225	0.590	51000	0.681	0.022	0.085	0.003	0.0597	0.0019	0.51265	522	13	524	18	531	67	-0.4
9	#418	239	105	56	1.867	18000	0.684	0.028	0.085	0.003	0.0590	0.0026	0.3802	526	17	527	19	500	93	-0.2
10	#494	178	69	121	0.571	36000	0.694	0.032	0.086	0.004	0.0593	0.0022	0.59912	526	19	529	23	507	77	-0.6
11	#429	361	135	206	0.655	490000	0.713	0.031	0.088	0.004	0.0598	0.0019	0.6839	542	18	539	22	536	68	0.6
12	#557	702	253	203	1.247	69000	0.719	0.025	0.088	0.004	0.0608	0.0021	0.51902	546	15	540	20	575	76	1.1
13	#411	488	180	160	1.123	210000	0.720	0.027	0.088	0.004	0.0609	0.0020	0.55625	545	16	544	21	564	71	0.2
14	#438	194	48	125	0.387	123000	0.807	0.041	0.089	0.005	0.0676	0.0027	0.64904	585	23	549	29	755	86	6.2
15	#416	566	183	239	0.766	360000	0.775	0.026	0.090	0.003	0.0631	0.0020	0.43923	576	15	551	18	652	68	4.3
16	#409	236	67	118	0.573	180000	0.808	0.033	0.091	0.004	0.0664	0.0023	0.60869	595	19	558	25	751	74	6.2
17	#538	307	87	147	0.588	31000	0.859	0.064	0.093	0.008	0.0716	0.0044	0.63625	622	35	567	44	850	130	8.8
18	#512	917	315	227	1.386	103000	0.781	0.026	0.094	0.003	0.0614	0.0021	0.41811	581	15	578	21	589	74	0.5
19	#568	148	53	110	0.477	15000	0.777	0.029	0.094	0.004	0.0610	0.0021	0.55208	578	16	579	21	575	74	-0.2
20	#578	430	145	383	0.378	127000	0.812	0.030	0.095	0.004	0.0641	0.0021	0.45576	597	17	583	21	669	72	2.3
21	#414	818	290	408	0.711	970000	0.787	0.024	0.095	0.003	0.0609	0.0016	0.52731	586	14	585	17	590	58	0.2
22	#575	538	175	236	0.739	68000	0.781	0.026	0.096	0.004	0.0602	0.0018	0.50622	580	15	588	21	570	66	-1.4
23	#514	412	133	261	0.508	106000	0.808	0.028	0.095	0.004	0.0622	0.0019	0.54843	595	15	588	22	630	64	1.2
24	#434	433	142	274	0.519	180000	0.816	0.026	0.096	0.003	0.0625	0.0020	0.46477	600	14	589	18	638	67	1.8
25	#536	176	58	60	0.968	21000	0.809	0.038	0.097	0.004	0.0616	0.0022	0.63508	592	22	591	23	578	77	0.2
26	#488	1940	577	555	1.040	500000	0.825	0.047	0.097	0.007	0.0652	0.0036	0.57752	602	26	592	38	690	120	1.7
27	#519	764	253	451	0.561	240000	0.791	0.027	0.096	0.004	0.0613	0.0018	0.55957	586	15	593	21	594	63	-1.2
28	#580	534	180	155	1.167	26000	0.816	0.035	0.096	0.005	0.0625	0.0021	0.63956	600	21	593	27	628	72	1.2
29	#472	2207	750	365	2.055	180000	0.828	0.026	0.097	0.003	0.0637	0.0018	0.53416	607	14	593	19	678	62	2.3
30	#573	207	70	80	0.872	28000	0.836	0.035	0.097	0.004	0.0629	0.0022	0.53583	607	20	596	23	638	77	1.8
31	#507	363	121	324	0.373	66000	0.824	0.030	0.097	0.004	0.0623	0.0019	0.56871	604	16	597	20	637	65	1.2
32	#456	125	44	61	0.722	17000	0.816	0.036	0.098	0.004	0.0613	0.0022	0.58085	595	20	602	24	566	76	-1.2
33	#495	190	63	66	0.954	38000	0.819	0.036	0.098	0.004	0.0608	0.0021	0.60349	595	20	602	24	559	76	-1.2
34	#540	137	45	54	0.822	19400	0.823	0.034	0.098	0.004	0.0636	0.0025	0.53442	601	19	602	23	617	80	-0.2
35	#428	842	284	209	1.359	440000	0.830	0.032	0.098	0.004	0.0629	0.0020	0.58763	613	19	602	22	645	69	1.8
36	#553	226	74	96	0.766	20000	0.846	0.037	0.098	0.004	0.0640	0.0022	0.58801	613	20	602	26	676	74	1.8
37	#450	262	93	96	0.978	30000	0.832	0.029	0.098	0.004	0.0617	0.0018	0.59068	610	16	603	21	624	65	1.1
38	#490	334	115	112	1.025	77000	0.816	0.033	0.099	0.004	0.0592	0.0017	0.56941	597	19	605	23	545	64	-1.3
39	#518	504	163	225	0.723	108000	0.825	0.033	0.099	0.004	0.0611	0.0021	0.48557	602	18	605	23	575	74	-0.5
40	#497	520	171	176	0.973	47000	0.837	0.038	0.099	0.004	0.0623	0.0019	0.71328	607	20	605	26	620	62	0.3
41	#554	853	281	372	0.756	191000	0.851	0.027	0.099	0.003	0.0634	0.0020	0.42523	622	15	605	19	677	69	2.7
42	#460	1284	380	477	0.797	540000	0.864	0.028	0.099	0.004	0.0643	0.0021	0.48005	629	16	605	21	690	71	3.8
43	#583	167	54	93	0.579	22000	0.837	0.033	0.099	0.004	0.0633	0.0022	0.6054	609	18	608	26	625	75	0.2
44	#508	635	213	126	1.688	62000	0.848	0.034	0.100	0.004	0.0625	0.0021	0.58866	616	19	610	23	620	71	1.0
45	#477	244	84	100	0.846	60000	0.829	0.033	0.100	0.004	0.0606	0.0020	0.54812	603	18	612	22	559	71	-1.5
46	#453	119	41	83	0.494	156000	0.849	0.032	0.100	0.004	0.0633	0.0022	0.61648	615	17	612	22	626	72	0.5
47	#417	835	283	162	1.749	220000	0.839	0.028	0.100	0.004	0.0622	0.0017	0.63064	617	16	612	21	636	61	0.8

48	#410	154	46	58	0.787	69000	0.894	0.045	0.101	0.005	0.0656	0.0030	0.41883	641	25	615	27	707	99	4.1
49	#430	108	36	14	2.655	3700	0.846	0.043	0.101	0.004	0.0625	0.0031	0.37899	608	23	616	24	570	110	-1.3
50	#473	882	290	212	1.372	50000	0.861	0.028	0.100	0.003	0.0630	0.0018	0.5666	628	15	616	20	662	62	1.9
51	#436	870	276	311	0.889	140000	0.848	0.024	0.101	0.003	0.0621	0.0019	0.47239	619	13	620	19	626	63	-0.2
52	#571	432	139	129	1.070	29000	0.866	0.036	0.101	0.004	0.0630	0.0021	0.57718	626	20	620	24	651	74	1.0
53	#577	557	193	147	1.311	44000	0.871	0.045	0.101	0.005	0.0631	0.0026	0.60147	629	25	620	29	665	90	1.4
54	#516	212	69	107	0.643	55000	0.875	0.035	0.101	0.004	0.0639	0.0023	0.54116	629	19	621	25	653	74	1.3
55	#586	176	59	68	0.872	20000	0.834	0.037	0.102	0.005	0.0598	0.0021	0.60152	606	20	626	26	545	76	-3.3
56	#469	465	157	52	3.041	48000	0.843	0.034	0.102	0.004	0.0614	0.0023	0.2846	610	19	628	25	550	77	-3.0
57	#515	867	269	236	1.140	56000	0.846	0.028	0.103	0.004	0.0608	0.0019	0.55504	615	16	629	24	576	67	-2.3
58	#476	77	24	56	0.439	31000	0.885	0.037	0.104	0.004	0.0638	0.0024	0.54183	634	20	634	23	634	77	0.0
59	#511	225	70	62	1.124	28000	0.887	0.036	0.104	0.005	0.0629	0.0023	0.56257	633	20	635	26	618	80	-0.3
60	#533	1002	313	293	1.068	75000	0.881	0.031	0.105	0.004	0.0628	0.0021	0.44305	637	16	639	22	636	73	-0.3
61	#534	712	218	188	1.162	30000	0.940	0.036	0.106	0.005	0.0664	0.0023	0.57083	670	20	648	27	763	75	3.3
62	#433	149	50	66	0.758	50000	0.893	0.035	0.107	0.005	0.0627	0.0021	0.50847	639	19	650	26	617	74	-1.7
63	#496	386	116	89	1.303	73000	0.976	0.049	0.106	0.006	0.0677	0.0029	0.57479	682	25	650	32	795	91	4.7
64	#475	153	51	31	1.618	26000	0.901	0.045	0.107	0.004	0.0622	0.0029	0.43247	643	24	651	23	589	99	-1.2
65	#471	191	61	106	0.573	64000	0.889	0.036	0.107	0.005	0.0617	0.0018	0.67572	636	20	653	26	613	64	-2.7
66	#548	139	38	259	0.147	72000	0.904	0.032	0.107	0.004	0.0622	0.0021	0.45832	646	17	654	24	619	75	-1.2
67	#592	488	151	215	0.704	55000	0.921	0.043	0.107	0.005	0.0636	0.0022	0.67628	652	23	654	29	647	72	-0.3
68	#574	202	67	61	1.106	21000	0.910	0.041	0.108	0.005	0.0612	0.0023	0.55544	649	22	656	26	593	83	-1.1
69	#447	1980	620	569	1.090	280000	0.924	0.027	0.108	0.004	0.0636	0.0018	0.56813	664	15	656	20	673	58	1.2
70	#451	95	32	20	1.569	29000	0.891	0.045	0.108	0.004	0.0614	0.0031	0.36359	634	24	658	26	520	100	-3.8
71	#509	304	91	58	1.556	37000	0.917	0.038	0.108	0.004	0.0634	0.0023	0.54256	649	20	658	25	638	79	-1.4
72	#584	165	51	34	1.496	6100	0.914	0.041	0.109	0.005	0.0632	0.0024	0.5722	650	22	662	28	609	81	-1.8
73	#454	708	211	185	1.143	101000	0.960	0.041	0.109	0.005	0.0647	0.0022	0.66214	674	21	666	29	697	73	1.2
74	#588	993	316	218	1.450	97000	0.932	0.040	0.110	0.005	0.0620	0.0019	0.61138	665	22	670	28	625	68	-0.8
75	#555	157	51	69	0.736	41000	0.932	0.035	0.110	0.004	0.0627	0.0020	0.51283	667	19	672	24	647	71	-0.7
76	#569	208	64	88	0.732	33000	0.933	0.042	0.111	0.005	0.0623	0.0020	0.67216	659	22	673	28	612	70	-2.1
77	#492	783	210	247	0.851	26000	0.973	0.043	0.111	0.005	0.0633	0.0022	0.60001	681	22	679	31	659	76	0.3
78	#493	305	88	52	1.707	42000	0.971	0.045	0.112	0.005	0.0644	0.0025	0.48063	676	23	680	28	649	83	-0.6
79	#581	772	228	177	1.289	72000	0.960	0.042	0.112	0.005	0.0631	0.0021	0.62301	671	22	681	28	646	69	-1.5
80	#535	91	28	34	0.836	5100	0.939	0.043	0.112	0.005	0.0622	0.0024	0.56497	661	23	682	28	595	83	-3.2
81	#457	163	48	87	0.556	49000	0.969	0.045	0.112	0.005	0.0633	0.0023	0.6224	678	24	683	26	640	75	-0.7
82	#513	569	168	114	1.469	43000	0.954	0.037	0.113	0.005	0.0610	0.0018	0.68098	669	19	686	26	581	61	-2.5
83	#470	867	266	222	1.198	113000	0.991	0.041	0.114	0.005	0.0645	0.0019	0.63321	686	21	692	28	702	65	-0.9
84	#539	77	24	49	0.482	12900	0.947	0.042	0.114	0.005	0.0628	0.0027	0.43063	667	22	694	29	601	89	-4.0
85	#579	103	30	39	0.785	5500	0.973	0.041	0.115	0.005	0.0631	0.0023	0.48131	681	21	696	25	645	77	-2.2
86	#587	252	76	63	1.191	12000	0.965	0.038	0.115	0.005	0.0626	0.0022	0.50811	679	20	700	27	617	75	-3.1
87	#427	149	45	40	1.139	17000	0.998	0.039	0.116	0.004	0.0625	0.0021	0.45952	691	19	704	24	615	74	-1.9
88	#437	376	104	41	2.544	71000	1.076	0.039	0.121	0.004	0.0652	0.0022	0.48909	733	19	735	25	707	72	-0.3
89	#478	804	219	190	1.154	260000	1.144	0.042	0.126	0.004	0.0670	0.0022	0.54613	767	19	763	25	784	67	0.5
90	#572	545	145	113	1.277	33000	1.105	0.052	0.127	0.006	0.0662	0.0023	0.65506	746	26	764	35	727	71	-2.4
91	#455	923	236	183	1.292	500000	1.139	0.047	0.126	0.005	0.0659	0.0018	0.72354	767	24	765	31	754	58	0.3
92	#528	623	147	90	1.625	40000	1.179	0.054	0.129	0.006	0.0670	0.0023	0.6178	782	26	780	34	794	71	0.3
93	#498	708	175	202	0.868	164000	1.304	0.061	0.131	0.006	0.0725	0.0024	0.67324	834	26	792	33	936	70	5.0
94	#589	997	193	109	1.765	19000	1.725	0.067	0.172	0.007	0.0742	0.0023	0.64363	1001	26	1018	39	991	64	-2.7
95	#591	351	64	21	2.993	8000	1.917	0.088	0.185	0.008	0.0766	0.0029	0.52088	1062	30	1088	42	1026	79	-6.0
96	#530	589	64	50	1.294	26000	5.010	0.200	0.320	0.013	0.1167	0.0039	0.52214	1798	34	1773	64	1847	62	4.0
97	#576	593	56	44	1.287	90000	5.810	0.350	0.354	0.022	0.1218	0.0058	0.60386	1898	52	1940	100	1901	88	-2.1
98	#590	684	70	70	1.002	73000	5.990	0.240	0.370	0.015	0.1205	0.0039	0.57469	1950	36	2006	70	1905	60	-5.3
99	#491	1377	143	111	1.293	210000	5.560	0.210	0.345	0.014	0.1180	0.0032	0.72121	1897	33	1895	65	1907	50	0.6
100	#529	683	71	70	1.013	148000	5.730	0.230	0.354	0.015	0.1206	0.0039	0.58845	1911	36	1943	73	1911	59	-1.7
101	#520	421	42	46	0.915	55000	6.070	0.240	0.370	0.015	0.1213	0.0042	0.55183	1960	36	2004	70	1917	63	-4.5
102	#531	724	77	78	0.987	14000	5.610	0.230	0.343	0.014	0.1197	0.0038	0.55594	1897	36	1883	65	1918	60	1.8
103	#585	708	71	91	0.787	-16000	5.850	0.230	0.357	0.014	0.1202	0.0034	0.62986	1929	34	1950	66	1926	50	-1.2

104	#551	224	22	18	1.236	35000	6.330	0.260	0.382	0.017	0.1214	0.0043	0.50208	1993	37	2065	76	1934	66	-6.8
105	#556	875	97	87	1.116	39000	5.380	0.200	0.330	0.013	0.1207	0.0034	0.63886	1857	32	1818	63	1940	52	6.3
106	#570	786	82	68	1.205	97000	5.750	0.220	0.350	0.013	0.1216	0.0038	0.57858	1927	34	1922	61	1943	55	1.1
107	#499	492	51	104	0.484	102000	6.020	0.240	0.357	0.014	0.1223	0.0035	0.6633	1951	36	1967	71	1946	53	-1.1
108	#440	832	81	81	0.993	320000	5.840	0.210	0.352	0.015	0.1214	0.0033	0.7044	1940	33	1931	69	1954	51	1.2
109	#415	1307	131	122	1.073	880000	5.780	0.220	0.342	0.013	0.1227	0.0033	0.70574	1919	35	1880	60	1954	46	3.8
110	#560	1649	173	119	1.455	105000	5.820	0.220	0.352	0.014	0.1221	0.0034	0.64091	1939	35	1937	68	1960	54	1.2
111	#558	946	98	76	1.281	146000	5.830	0.230	0.349	0.015	0.1225	0.0038	0.66103	1926	36	1909	73	1969	57	3.0
112	#552	502	55	43	1.294	58000	5.840	0.210	0.349	0.013	0.1244	0.0039	0.59426	1946	32	1916	63	1992	54	3.8
113	#467	1461	143	166	0.858	400000	6.050	0.240	0.353	0.015	0.1266	0.0034	0.73218	1955	36	1936	72	2001	48	3.2
114	#547	1623	144	152	0.951	70000	6.340	0.260	0.372	0.017	0.1264	0.0040	0.69523	1987	39	2010	81	2004	57	-0.3
115	#413	966	93	59	1.576	930000	6.140	0.290	0.356	0.015	0.1282	0.0057	0.42905	1979	42	1950	72	2010	82	3.0
116	#567	425	41	78	0.528	50000	6.700	0.240	0.379	0.016	0.1326	0.0040	0.60725	2057	32	2048	74	2100	55	2.5
117	#479	855	82	72	1.138	77000	7.460	0.310	0.395	0.016	0.1369	0.0045	0.6435	2130	40	2137	78	2128	57	-0.4
118	#480	441	40	101	0.392	410000	7.380	0.330	0.396	0.017	0.1350	0.0038	0.73231	2135	42	2142	83	2129	48	-0.6
119	#487	400	37	37	1.000	40000	7.310	0.310	0.388	0.017	0.1385	0.0044	0.64614	2128	37	2108	82	2184	58	3.5
120	#527	317	31	80	0.387	34000	7.420	0.280	0.387	0.017	0.1400	0.0039	0.6939	2163	31	2092	78	2192	51	4.6
121	#459	579	53	32	1.647	176000	8.310	0.310	0.420	0.014	0.1446	0.0048	0.55817	2253	34	2259	65	2244	58	-0.7
122	#412	2891	266	213	1.246	3800000	9.770	0.410	0.438	0.019	0.1620	0.0064	0.50863	2401	39	2334	87	2463	71	5.2
123	#452	4320	282	230	1.229	2400000	13.780	0.590	0.527	0.027	0.1970	0.0110	0.38776	2720	40	2710	110	2749	81	1.4
124	#431	1153	75	73	1.019	1020000	15.290	0.620	0.563	0.025	0.2047	0.0072	0.62852	2810	42	2839	100	2796	52	-1.5
125	#468	1253	87	59	1.488	400000	18.500	1.100	0.563	0.036	0.2420	0.0130	0.53531	2994	58	2880	160	3113	83	7.5
Analyses disc. >10%																				
1	#432	734	151	321	0.469	170000	1.134	0.046	0.099	0.004	0.0851	0.0031	0.53157	756	22	607	25	1238	72	19.7
2	#449	328	89	35	2.506	54000	1.435	0.055	0.107	0.004	0.0987	0.0032	0.56063	892	23	651	22	1547	62	27.0
3	#510	349	81	87	0.923	48000	1.316	0.066	0.118	0.006	0.0839	0.0037	0.54408	834	28	712	32	1184	88	14.6
4	#517	330	68	48	1.410	21000	1.810	0.120	0.117	0.006	0.1115	0.0063	0.45696	1002	44	715	35	1660	110	28.6
5	#549	272	66	18	3.554	5700	1.466	0.077	0.128	0.006	0.0861	0.0041	0.4981	895	32	770	36	1207	97	14.0
6	#500	522	65	94	0.695	34000	3.670	0.160	0.242	0.011	0.1117	0.0036	0.66299	1538	36	1391	59	1786	60	22.1
7	#435	671	66	68	0.961	147000	4.110	0.180	0.259	0.012	0.1161	0.0040	0.67953	1627	38	1475	62	1831	64	19.4
8	#474	1156	130	233	0.559	380000	4.510	0.160	0.273	0.010	0.1198	0.0034	0.65011	1713	31	1553	54	1914	53	18.9
9	#537	1505	128	157	0.814	110000	5.360	0.390	0.316	0.024	0.1282	0.0064	0.74333	1815	64	1740	120	1989	88	12.5
10	#489	1091	106	248	0.429	1120000	6.330	0.280	0.344	0.016	0.1360	0.0043	0.76293	2010	41	1901	75	2145	55	11.4
11	#559	493	51	80	0.631	55000	7.350	0.330	0.333	0.017	0.1631	0.0054	0.68551	2139	41	1839	80	2455	60	25.1
12	#448	891	67	132	0.510	840000	9.420	0.450	0.366	0.018	0.1897	0.0054	0.76266	2322	50	1975	86	2726	49	27.5
13	#532	961	69	163	0.423	600000	20.910	0.800	0.560	0.029	0.2770	0.0120	0.61997	3128	40	2830	120	3301	56	14.3
Sample OS9/2 – migmatitic paragneiss of the SMB middle unit																				
1	#93	73	138	314	0.440	600000	0.434	0.015	0.056	0.002	0.0558	0.0016	0.4728	365	11	354	10	405	64	3.0
2	#180	4	7	771	0.009	110000	0.435	0.012	0.059	0.002	0.0534	0.0013	0.59052	366	9	368	9	327	52	-0.5
3	#38	2	3	574	0.005	-150000	0.449	0.013	0.060	0.002	0.0540	0.0013	0.48024	375	9	377	9	350	54	-0.4
4	#28	3	5	698	0.007	200000	0.448	0.013	0.061	0.002	0.0538	0.0013	0.51874	375	9	378	10	345	57	-1.0
5	#13	3	5	520	0.009	-220000	0.455	0.014	0.061	0.002	0.0545	0.0015	0.53564	380	10	379	11	367	61	0.3
6	#173	5	6	604	0.010	-400000	0.457	0.016	0.061	0.002	0.0544	0.0016	0.61256	381	11	380	12	369	66	0.4
7	#114	4	6	727	0.008	37000000	0.459	0.013	0.061	0.002	0.0544	0.0014	0.60992	382	9	381	11	366	55	0.4
8	#10	6	8	1163	0.007	460000	0.459	0.013	0.061	0.002	0.0542	0.0013	0.42446	383	9	382	10	357	55	0.3
9	#97	5	8	619	0.013	150000	0.459	0.013	0.061	0.002	0.0541	0.0013	0.57056	383	9	383	10	361	54	0.0
10	#16	3	5	781	0.007	22000000	0.461	0.013	0.061	0.002	0.0542	0.0013	0.56748	384	9	383	10	361	54	0.2
11	#147	4	6	917	0.007	400000	0.459	0.013	0.061	0.002	0.0544	0.0013	0.52415	383	9	383	10	367	54	-0.1
12	#170	2	3	528	0.005	900000	0.458	0.014	0.061	0.002	0.0543	0.0014	0.55531	382	10	384	10	359	57	-0.3
13	#195	3	5	540	0.010	500000	0.460	0.014	0.061	0.002	0.0539	0.0014	0.5805	383	10	384	10	342	55	-0.1
14	#174	2	4	643	0.006	-900000	0.467	0.014	0.061	0.002	0.0552	0.0014	0.52751	388	10	384	10	397	56	1.1
15	#74	2	4	598	0.006	900000	0.458	0.014	0.062	0.002	0.0542	0.0014	0.54139	382	10	385	10	358	56	-0.8
16	#128	2	4	420	0.008	160000	0.458	0.014	0.062	0.002	0.0536	0.0014	0.5191	382	10	385	10	336	58	-0.7
17	#55	3	4	621	0.007	1090000	0.466	0.016	0.062	0.002	0.0549	0.0016	0.56894	387	11	385	12	387	66	0.6
18	#155	3	4	539	0.008	260000	0.462	0.014	0.062	0.002	0.0544	0.0015	0.58791	385	10	385	11	358	59	-0.2

19	#189	4	6	708	0.008	120000	0.462	0.013	0.062	0.002	0.0538	0.0013	0.52939	385	9	386	10	344	54	-0.3
20	#71	7	11	553	0.019	-170000	0.458	0.014	0.062	0.002	0.0541	0.0014	0.58408	382	10	386	10	354	56	-1.1
21	#20	3	5	672	0.008	700000	0.462	0.013	0.062	0.002	0.0540	0.0013	0.54248	385	9	386	10	348	54	-0.4
22	#32	2	3	515	0.006	210000	0.462	0.013	0.062	0.002	0.0540	0.0013	0.4942	385	9	387	10	354	54	-0.4
23	#132	2	3	548	0.006	-5000	0.461	0.014	0.062	0.002	0.0539	0.0014	0.46593	384	10	387	10	347	57	-0.7
24	#30	4	6	468	0.014	120000	0.464	0.016	0.062	0.002	0.0543	0.0016	0.54898	386	11	387	12	362	65	-0.2
25	#59	8	14	1028	0.013	2120000	0.464	0.013	0.062	0.002	0.0548	0.0013	0.54726	386	9	387	10	383	55	-0.2
26	#197	10	14	651	0.022	-370000	0.467	0.015	0.062	0.002	0.0547	0.0016	0.49089	388	10	388	12	368	64	0.2
27	#137	5	9	914	0.010	120000	0.464	0.013	0.062	0.002	0.0541	0.0012	0.5539	386	9	388	10	358	52	-0.5
28	#198	4	2	511	0.004	-700000	0.459	0.015	0.062	0.002	0.0534	0.0016	0.49513	382	11	388	12	326	69	-1.6
29	#148	4	7	1212	0.006	600000	0.466	0.013	0.062	0.002	0.0545	0.0013	0.53772	388	9	388	10	371	54	-0.1
30	#154	8	14	1089	0.013	200000	0.463	0.013	0.062	0.002	0.0540	0.0013	0.53909	386	9	388	10	350	53	-0.6
31	#177	2	5	440	0.011	-32000	0.468	0.014	0.062	0.002	0.0546	0.0014	0.49502	388	10	388	10	372	58	0.0
32	#95	2	4	610	0.007	640000	0.466	0.013	0.062	0.002	0.0542	0.0013	0.57037	388	9	388	10	368	54	-0.2
33	#172	3	3	536	0.005	10000	0.470	0.014	0.062	0.002	0.0550	0.0014	0.54911	391	10	388	10	390	58	0.7
34	#76	3	5	612	0.008	210000	0.469	0.014	0.062	0.002	0.0549	0.0014	0.55914	390	9	389	11	391	57	0.3
35	#75	2	3	988	0.003	-100000	0.461	0.013	0.062	0.002	0.0541	0.0013	0.57103	384	9	389	10	361	54	-1.2
36	#67	1	2	436	0.005	-270000	0.465	0.015	0.062	0.002	0.0544	0.0015	0.52974	386	10	389	11	358	60	-0.8
37	#194	2	4	580	0.007	-400000	0.467	0.013	0.062	0.002	0.0541	0.0013	0.54997	388	9	390	10	357	56	-0.3
38	#50	5	5	664	0.008	800000	0.464	0.013	0.062	0.002	0.0545	0.0013	0.61067	388	9	390	10	374	52	-0.4
39	#153	7	11	569	0.019	-100000	0.469	0.015	0.062	0.002	0.0550	0.0016	0.50432	389	10	390	12	381	63	-0.2
40	#192	2	3	478	0.005	-700000	0.460	0.014	0.063	0.002	0.0530	0.0014	0.51429	384	10	391	10	309	58	-1.9
41	#53	2	3	468	0.007	-500000	0.469	0.014	0.063	0.002	0.0546	0.0014	0.60802	390	10	391	10	375	55	-0.1
42	#176	3	5	637	0.007	-610000	0.464	0.014	0.063	0.002	0.0537	0.0014	0.48588	386	10	391	10	341	59	-1.1
43	#190	2	3	469	0.007	-3000	0.458	0.015	0.063	0.002	0.0528	0.0015	0.45907	383	10	391	11	297	62	-2.3
44	#72	5	9	1094	0.008	-560000	0.468	0.013	0.063	0.002	0.0544	0.0013	0.4953	389	9	392	10	376	56	-0.7
45	#199	1	2	372	0.006	0	0.468	0.015	0.063	0.002	0.0537	0.0014	0.61349	389	10	392	11	329	59	-0.8
46	#115	1	3	644	0.004	-2200000	0.465	0.015	0.063	0.002	0.0532	0.0014	0.54535	387	10	392	11	321	61	-1.3
47	#168	2	4	341	0.011	20000	0.480	0.023	0.063	0.003	0.0557	0.0022	0.60701	396	16	392	17	403	86	1.0
48	#77	4	4	573	0.006	-110000	0.470	0.014	0.063	0.002	0.0547	0.0014	0.51105	390	10	392	11	373	58	-0.6
49	#12	1	2	250	0.007	-140000	0.482	0.016	0.063	0.002	0.0555	0.0017	0.42364	397	11	394	11	387	66	0.9
50	#91	0	1	173	0.004	-2100000	0.471	0.017	0.063	0.002	0.0542	0.0018	0.45321	389	12	396	12	331	70	-1.7
51	#196	2	4	345	0.011	41000	0.478	0.018	0.063	0.002	0.0543	0.0017	0.57475	394	12	396	13	348	68	-0.4
52	#35	1	2	321	0.006	700000	0.478	0.015	0.064	0.002	0.0547	0.0014	0.55328	396	10	397	11	378	58	-0.1
53	#110	2	3	400	0.006	-380000	0.469	0.015	0.063	0.002	0.0540	0.0016	0.47026	389	10	397	12	339	66	-1.9
54	#73	2	2	358	0.007	-400000	0.474	0.015	0.064	0.002	0.0543	0.0014	0.5255	392	10	398	11	360	59	-1.4
55	#107	1	2	302	0.007	-500000	0.465	0.014	0.064	0.002	0.0528	0.0015	0.41611	387	10	400	11	303	61	-3.4
56	#57	1	2	231	0.007	270000	0.483	0.018	0.064	0.002	0.0549	0.0017	0.61259	398	12	400	13	375	66	-0.6
57	#51	1	2	318	0.006	350000	0.489	0.016	0.065	0.002	0.0551	0.0015	0.59566	403	11	404	11	394	59	-0.2
58	#131	3	3	249	0.011	170000	0.488	0.015	0.065	0.002	0.0544	0.0015	0.53326	403	11	405	11	361	59	-0.5
59	#68	1	1	226	0.006	42000	0.488	0.016	0.065	0.002	0.0551	0.0016	0.45683	402	11	405	11	384	64	-0.8
60	#179	1	1	213	0.007	-64000	0.485	0.016	0.065	0.002	0.0543	0.0017	0.25393	401	11	406	11	350	70	-1.2
61	#188	2	3	370	0.007	500000	0.496	0.026	0.066	0.002	0.0542	0.0026	0.37451	408	18	411	15	353	110	-0.7
62	#112	62	78	328	0.236	-1280000	0.530	0.017	0.069	0.002	0.0553	0.0014	0.63901	431	11	432	13	400	58	-0.2
63	#37	58	71	500	0.143	-300000	0.542	0.020	0.070	0.002	0.0559	0.0017	0.6627	438	13	435	14	425	67	0.7
64	#31	8	10	354	0.029	200000	0.546	0.018	0.071	0.002	0.0561	0.0015	0.60988	440	12	439	12	432	59	0.2
65	#200	215	220	623	0.354	700000	0.548	0.017	0.071	0.002	0.0560	0.0015	0.58101	442	11	440	13	424	59	0.7
66	#191	43	60	272	0.221	80000	0.581	0.018	0.074	0.002	0.0562	0.0014	0.59923	464	11	460	12	437	56	0.7
67	#151	95	119	596	0.199	300000	0.584	0.017	0.076	0.002	0.0563	0.0014	0.56654	466	11	470	13	441	56	-0.7
68	#127	43	51	155	0.330	-30000	0.636	0.024	0.078	0.002	0.0589	0.0021	0.23845	498	15	484	14	549	83	2.8
69	#90	35	42	17	2.527	-44000	0.635	0.048	0.079	0.003	0.0594	0.0046	0.15187	483	30	488	17	380	150	-1.0
70	#157	2	2	252	0.008	100000	0.616	0.021	0.079	0.003	0.0569	0.0016	0.59267	486	14	489	15	460	62	-0.6
71	#150	91	93	393	0.237	5000000	0.628	0.021	0.079	0.002	0.0575	0.0015	0.66423	494	13	491	14	486	58	0.5
72	#111	249	244	587	0.415	-120000	0.623	0.019	0.081	0.002	0.0560	0.0014	0.66072	490	12	498	14	427	56	-1.7
73	#33	45	59	183	0.320	-15000	0.664	0.021	0.083	0.002	0.0583	0.0016	0.43094	514	13	511	13	512	59	0.7

74	#133	33	45	98	0.457	223000	0.677	0.024	0.085	0.002	0.0579	0.0018	0.43327	521	14	525	14	479	66	-0.7
75	#58	22	25	89	0.284	20000	0.677	0.025	0.085	0.003	0.0585	0.0020	0.41594	522	15	527	16	504	72	-1.0
76	#119	57	71	101	0.702	-90000	0.690	0.025	0.086	0.003	0.0582	0.0019	0.35339	530	15	533	15	478	71	-0.6
77	#98	407	404	712	0.567	3100000	0.702	0.023	0.087	0.003	0.0588	0.0015	0.69782	538	13	536	17	539	58	0.4
78	#19	170	214	267	0.802	130000	0.698	0.021	0.087	0.003	0.0584	0.0015	0.58446	536	13	538	15	517	55	-0.4
79	#138	48	62	82	0.751	-20000	0.716	0.026	0.088	0.003	0.0589	0.0020	0.31874	544	15	545	15	509	74	-0.2
80	#129	126	151	188	0.803	160000	0.727	0.028	0.089	0.003	0.0596	0.0021	0.49601	552	16	548	18	544	76	0.7
81	#70	92	113	206	0.546	-900000	0.712	0.023	0.089	0.003	0.0587	0.0017	0.52888	544	14	550	16	513	62	-1.2
82	#48	54	66	168	0.395	125000	0.721	0.025	0.090	0.003	0.0589	0.0017	0.54462	547	14	552	15	517	63	-0.9
83	#169	21	25	39	0.659	-20000	0.736	0.033	0.091	0.003	0.0588	0.0024	0.34708	555	20	560	16	490	88	-0.9
84	#92	82	104	44	2.357	187000	0.732	0.030	0.091	0.003	0.0585	0.0023	0.19613	554	18	563	16	481	85	-1.6
85	#40	194	211	257	0.823	-600000	0.815	0.024	0.099	0.003	0.0603	0.0016	0.47185	603	14	605	16	586	56	-0.4
86	#117	199	221	157	1.408	-120000	0.846	0.027	0.102	0.003	0.0597	0.0016	0.48328	620	15	629	17	560	61	-1.5
87	#156	152	91	211	0.433	700000	1.596	0.056	0.147	0.005	0.0788	0.0021	0.69617	962	22	883	26	1136	55	8.2
88	#14	226	155	323	0.480	240000	1.626	0.059	0.156	0.005	0.0753	0.0023	0.58846	977	23	932	29	1070	59	4.6
89	#29	78	56	184	0.303	180000	1.647	0.062	0.160	0.006	0.0748	0.0023	0.63656	985	23	954	30	1048	61	3.1
90	#99	32	19	104	0.180	850000	2.258	0.065	0.203	0.006	0.0802	0.0019	0.59593	1195	21	1191	30	1187	48	-0.3
91	#49	226	92	304	0.302	560000	4.330	0.150	0.290	0.011	0.1087	0.0030	0.73307	1693	29	1640	54	1766	52	7.1
92	#178	2487	948	953	0.995	1400000	5.400	0.170	0.324	0.010	0.1202	0.0030	0.67741	1883	27	1808	50	1958	48	7.7
93	#17	360	122	171	0.709	400000	6.180	0.180	0.363	0.011	0.1227	0.0030	0.63398	1998	25	1995	50	1990	45	-0.3
94	#120	1003	303	319	0.949	-470000	6.480	0.190	0.376	0.011	0.1247	0.0028	0.71405	2037	25	2053	50	2013	40	-2.0
95	#139	317	106	132	0.807	110000	6.070	0.180	0.346	0.010	0.1265	0.0030	0.70585	1981	25	1912	48	2042	43	6.4
96	#159	242	80	127	0.625	-400000	6.480	0.180	0.368	0.010	0.1277	0.0031	0.60713	2038	24	2020	49	2052	42	1.6
97	#36	119	42	70	0.601	-200000	6.030	0.190	0.345	0.011	0.1275	0.0036	0.55946	1980	29	1905	54	2058	52	7.4
98	#54	82	22	106	0.213	130000	6.350	0.200	0.351	0.011	0.1328	0.0034	0.64941	2023	28	1937	52	2121	46	8.7
99	#160	673	191	409	0.466	7000000	9.750	0.430	0.429	0.019	0.1655	0.0064	0.58224	2403	39	2296	87	2496	66	8.0
100	#94	628	164	224	0.732	140000	11.500	0.310	0.484	0.013	0.1728	0.0039	0.69063	2563	25	2539	57	2579	37	1.6
101	#34	156	41	190	0.216	170000	11.240	0.340	0.470	0.014	0.1741	0.0046	0.5053	2539	28	2478	60	2586	45	4.2
102	#100	381	107	191	0.564	-800000	11.390	0.340	0.474	0.013	0.1738	0.0039	0.74943	2547	28	2494	58	2590	37	3.7
Analyses disc. >10%																				
1	#80	32	3	593	0.005	-190000	0.552	0.029	0.062	0.003	0.0654	0.0035	0.32335	445	19	388	17	740	120	12.8
2	#135	12	1	89	0.015	71000	0.694	0.027	0.067	0.002	0.0758	0.0028	0.33229	531	16	416	12	1045	78	21.7
3	#108	6	7	562	0.012	-700000	0.632	0.021	0.070	0.002	0.0661	0.0017	0.62673	496	13	433	12	776	57	12.7
4	#9	27	19	552	0.034	700000	0.846	0.033	0.080	0.003	0.0760	0.0025	0.59299	621	19	497	18	1083	68	20.0
5	#113	91	117	479	0.244	12100000	0.819	0.024	0.081	0.002	0.0731	0.0019	0.55547	606	13	503	14	1001	52	16.9
6	#187	18	19	330	0.059	700000	0.911	0.031	0.096	0.003	0.0684	0.0018	0.65477	654	16	587	16	856	56	10.2
7	#60	40	30	300	0.101	230000	1.205	0.040	0.096	0.003	0.0913	0.0024	0.66791	799	18	591	17	1439	49	26.0
8	#116	115	89	255	0.351	-210000	1.531	0.049	0.120	0.004	0.0924	0.0024	0.65887	939	20	727	21	1459	49	22.6
9	#78	35	17	575	0.030	-330000	2.198	0.064	0.151	0.004	0.1061	0.0025	0.70479	1175	20	908	24	1719	42	22.7
10	#167	48	27	68	0.395	77000	2.049	0.071	0.154	0.005	0.0974	0.0030	0.44268	1128	25	924	28	1537	59	18.1
11	#149	95	61	181	0.337	1000000	1.857	0.063	0.169	0.005	0.0805	0.0022	0.66472	1060	23	1003	30	1186	56	15.4
12	#15	524	296	825	0.359	-13900000	2.107	0.061	0.184	0.005	0.0821	0.0019	0.70639	1149	20	1089	29	1244	46	12.5
13	#52	92	44	141	0.312	100000	2.721	0.087	0.194	0.006	0.1029	0.0026	0.72813	1328	24	1138	32	1659	46	31.4
14	#140	117	51	120	0.421	1170000	2.948	0.110	0.202	0.007	0.1058	0.0033	0.56778	1392	28	1186	39	1712	56	30.7
15	#96	368	150	101	1.482	440000	3.485	0.110	0.232	0.007	0.1081	0.0028	0.6912	1519	27	1345	37	1755	49	23.4
16	#130	311	169	287	0.587	140000	2.976	0.089	0.193	0.006	0.1113	0.0027	0.6722	1396	23	1136	30	1809	43	37.2
17	#118	247	106	176	0.601	-720000	4.100	0.170	0.265	0.012	0.1119	0.0039	0.66132	1646	35	1512	59	1820	65	16.9
18	#47	150	67	371	0.179	590000	2.814	0.092	0.182	0.006	0.1127	0.0027	0.79942	1356	26	1077	30	1832	44	41.2
19	#8	145	61	76	0.804	-200000	3.673	0.120	0.232	0.008	0.1138	0.0033	0.54351	1557	26	1340	39	1849	53	27.5
20	#134	539	204	420	0.485	-150000	4.047	0.130	0.254	0.009	0.1152	0.0030	0.71243	1643	26	1456	44	1879	49	22.5
21	#175	230	100	321	0.312	-110000	3.221	0.110	0.200	0.007	0.1165	0.0029	0.8191	1454	28	1172	37	1895	45	38.2
22	#27	197	86	288	0.299	-130000	4.081	0.130	0.241	0.008	0.1231	0.0033	0.65223	1647	25	1388	39	1990	47	30.3
23	#11	77	26	57	0.455	-180000	5.490	0.280	0.321	0.019	0.1230	0.0049	0.7611	1898	43	1794	91	1996	69	10.1
24	#193	15	5	11	0.488	30000	5.840	0.250	0.327	0.011	0.1276	0.0050	0.41644	1935	37	1819	54	2027	71	10.3
25	#87	223	76	176	0.428	220000	5.470	0.180	0.296	0.010	0.1341	0.0038	0.58071	1888	29	1669	48	2135	49	21.8

26	#171	288	132	574	0.230	130000	3.481	0.130	0.187	0.006	0.1344	0.0033	0.83717	1510	28	1101	34	2143	42	48.6
27	#89	31	12	571	0.022	-620000	3.560	0.210	0.182	0.009	0.1365	0.0038	0.9572	1479	50	1071	48	2164	50	50.5
28	#88	303	186	367	0.507	-270000	3.392	0.110	0.173	0.005	0.1426	0.0037	0.6986	1498	26	1026	30	2253	43	54.5
29	#109	339	107	325	0.329	20000	8.160	0.320	0.357	0.012	0.1650	0.0047	0.74104	2242	35	1963	57	2498	48	21.4
30	#79	746	210	734	0.286	-2900000	9.230	0.290	0.396	0.012	0.1691	0.0043	0.68793	2357	28	2154	59	2541	44	15.2
31	#7	398	150	597	0.251	-2000000	6.760	0.200	0.286	0.009	0.1704	0.0041	0.72127	2076	26	1617	43	2556	39	36.7
32	#152	536	131	529	0.247	-1360000	8.030	0.280	0.331	0.011	0.1745	0.0042	0.82496	2224	30	1837	52	2598	40	29.3
33	#136	133	41	273	0.151	-140000	9.530	0.320	0.392	0.014	0.1763	0.0046	0.76378	2384	31	2126	62	2610	43	18.5
34	#69	1510	386	538	0.717	20000	9.790	0.280	0.395	0.011	0.1813	0.0042	0.6946	2408	26	2141	52	2653	38	19.3